MALMÖ UNIVERSITY HEALTH AND SOCIETY DOCTORAL DISSERTATION 2016:3

ZAHRA EL-SCHICH

NOVEL IMAGING TECHNOLOGY AND TOOLS FOR BIOMARKER DETECTION IN CANCER

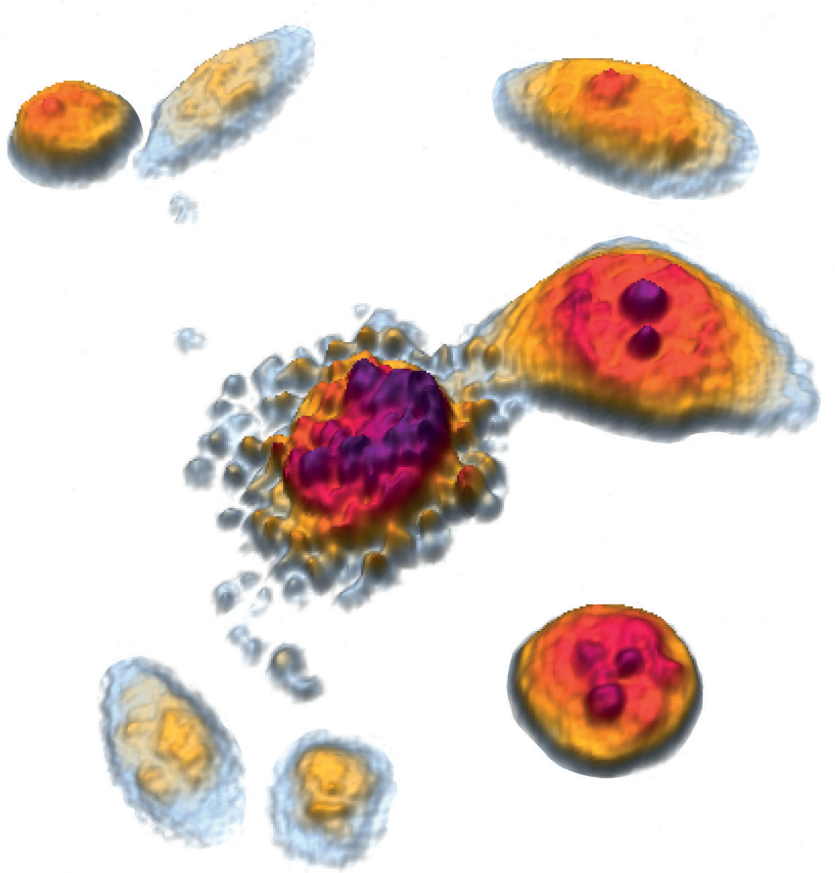

MALMÖ UNIVERSITY

NOVEL IMAGING TECHNOLOGY AND TOOLS FOR BIOMARKER DETECTION IN CANCER

Malmö University
Health and Society, Doctoral Dissertation 2016:3

Front illustration: Dying cells captured with digital holography microscopy.
www.phiab.se
ISBN 978-91-7104-660-4 (print)
ISBN 978-91-7104-661-1 (pdf)
ISSN 1653-5383
Holmbergs, Malmö 2016

ZAHRA EL-SCHICH

NOVEL IMAGING TECHNOLOGY AND TOOLS FOR BIOMARKER DETECTION IN CANCER

Malmö University, Sweden, 2016
Faculty of Health and Society
Department of Biomedical Science

Till min familj

”Research is to see what everybody else has seen,
and to think what nobody else has thought”
– Albert Szent-Gyorgyi

CONTENTS

ABBREVIATIONS

ALL	Acute lymphoblastic leukemia
AML	Acute myeloid leukemia
Apaf-1	Apoptotic protease activating factor 1
Bcl-2	B cell lymphoma 2
Bcl-X_L	B cell lymphoma extra large
BCR	B cell receptor
BM	Bone marrow
Pre-B cell	Precursor B cell
Pro-B cell	Progenitor B cell
Caspase	Cysteine aspartyl-specific protease
CD	Cluster of differentiation
CDKs	Cyclin dependent kinases
CLL	Chronic lymphocytic leukemia
CML	Chronic myeloid leukemia
DH	Digital holography
DLBCL	Diffuse large B cell lymphoma
FADD	FAS associated death domain containing protein
FL	Follicular lymphoma
Ig	Immunoglobulin
IGHV	Immunoglobulin heavy chain variable
LN	Lymph nodes
LYN	Lck/Yes novel protein tyrosine kinase
MCL	Mantle cell lymphoma
MIP	Molecular imprinting polymer
Neu5Ac	N-acetylneuraminic acid
Neu5Gc	N-glycolylneuraminic acid
NK	Natural killer

PB	Peripheral blood
PTK	Protein Tyrosine Kinase
PTP	Protein Tyrosine Phosphatase
SA	Sialic acid
ScFv	single-chain variable antibody fragments
SHP-1	SH2-domain containing phosphatase 1
SYK	Spleen tyrosine kinase
TNFR	Tumor necrosis factor receptor
ZAP70	Zeta chain associated protein kinase of 70 kDa

ABSTRACT

Cancer is a leading cause of death worldwide. Normally the balance between cell growth and cell death is strongly controlled. Chronic lymphocytic leukemia is an indolent disease that has a highly variable clinical course and is the most common hematological malignancy amongst adults in the Western countries. The protein tyrosine phosphatase SHP-1 is a key regulator that controls the intracellular phosphotyrosine level in lymphocytes by inhibiting the B cell receptor signals. We have compared the expression and activity of SHP-1 in chronic lymphocytic leukemia cells from lymph nodes with matched peripheral blood samples. The expression levels of SHP-1 were higher in peripheral blood, but the phosphatase activity in lymph nodes and peripheral blood did not differ significantly. All cells in the body normally present glycans on the cell surface, which are involved in cellular communication and in processes like cell differentiation, proliferation and infection, including protecting the cells from invaders and in cell-cell contacts. Sialic acid occurs on the terminal end of glycans, and the frequency of sialic acid expression is increased on metastatic cancer cells and overexpression controls tumor cell growth and cell differentiation. The availability of specific antibodies against sialic acid is limited. We have been screening sialic acid on cancer cells by using a molecular imprinting polymer technique. Our results show that sialic acid is expressed on chronic lymphocytic leukemia cell lines at different levels at the plasma membrane. Higher expression of sialic acid in the more aggressive chronic lymphocytic leukemia cell lines was observed. To analyze morphological changes of death cells, digital holographic microscopy was used. Digital holographic microscopy is an approach for label-free non-invasive 3D imaging of cultured cells. We have analyzed cell death of adherent cancer cells using digital holographic microscopy and developed it to analyze suspension cells by combining this technique with antibody based microassays. Digital holographic microscopy can be used for cell-death induced cell analysis of both adherent cells and suspension cells. This thesis takes us one step further in cancer research as regards developing techniques for screening circulating cancer cells in blood as well as for individualized treatment of cancer patients.

LIST OF ORIGINAL PAPERS

I. Bergh A.C., **El-Schich Z.**, Delfani P., Ohlsson L., Rósen A., Gjörloff Wingren A. B cell receptor signaling suppressor SHP-1 is active in CLL lymph node and peripheral blood. *Manuscript in preparation.*

II. **El-Schich Z.**, Mohammad A., Shinde S., Dizeyi N., Rosén A., Sellergren B., Gjörloff Wingren A. Different expression of glycans on leukemic cells - a screening with molecularly imprinted polymers targeting sialic acid. *Manuscript submitted for publication.*

III. **El-Schich Z**, Mölder A, Tassidis H, Härkönen P, Falck Miniotis M, Gjörloff Wingren A. Induction of morphological changes in death-induced cancer cells monitored by holographic microscopy. *Journal of Structural Biology.* 2015 3;189(3):207-12.

IV. **El-Schich Z**, Nilsson E, Gerdtsson AS, Wingren C, Gjörloff Wingren A. Interfacing antibody-based microarrays and digital holography enables label-free detection for loss of cell volume. *Future Science OA.* 2015(0):1-11.

Authors 'contributions

In paper I ZE designed the study, performed the experiments and analyzed the data. In paper II ZE designed the study, performed the experiments, analyzed the data and wrote the manuscript with contributions from the other authors. In paper III ZE designed the study, performed all the experiments, analyzed the data and wrote the paper with contributions from the other authors. In paper IV ZE performed the experiments, analyzed the data and wrote the paper with contributions from the other authors.

INTRODUCTION

Cancer is a leading cause of death worldwide (Torre *et al.* 2015). There are more than 100 types of human malignancies found in different organs (Hanahan & Weinberg 2000). Cancer is involved in morphological cellular transformation, uncontrolled cell proliferation, metastasis, dysregulation of apoptosis, invasion and angiogenesis (Fischer-Fodor *et al.* 2015; Lin & Karin 2007).

Metastasis is a complex multi-step process, were primary tumor cells migrate and metastasize to other organs in the body by the blood system and form secondary tumors (Chaffer & Weinberg 2011; Zimmer & Steeg 2015). However, metastasizing tumors lose their adhesion to other cells; they destroy and degrade the extracellular matrix and basement membrane and enter the blood system. Figure 1 shows a schematic drawing of tumor metastasis (Fidler 2003; Lu *et al.* 2012; van Horssen *et al.* 2013).

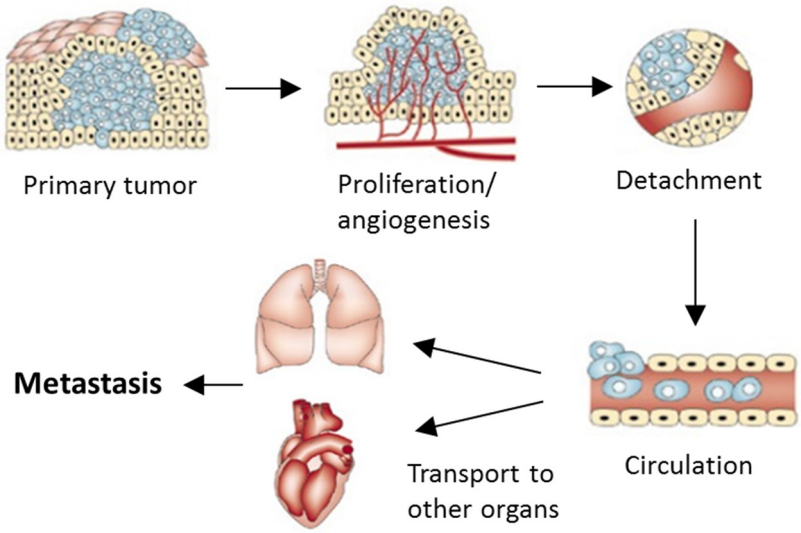

Figure 1. Schematic drawing of tumor metastasis. Modified from (Fidler 2003)

The balance between cell growth and cell death is strongly controlled (Gérard & Goldbeter 2014). Cell death occurs in different ways, through apoptosis or necrosis. Apoptosis is a thoroughly investigated mechanism that occurs normally in the body and plays a central role in development as well as in homeostasis and is necessary for removal of dysfunctional, mutated or tumor cells (Alibek *et al.* 2014; Taylor *et al.* 2008). Mutations of apoptotic genes promote disorders such as autoimmune diseases and cancer. Dying cells differ from viable cells in several aspects (Ashkenazi & Salvesen 2014). Apoptosis characterize a variety of morphological changes such as loss of cell membrane asymmetry and attachment, cell shrinkage, formation of small blebs, nuclear fragmentation, chromatin condensation, chromosomal DNA fragmentation and finally breakdown of the cell into several apoptotic bodies (Debatin 2004; Elmore 2007; Wong 2011).

Apoptosis

Apoptosis can be realized according to two different mechanisms, the intrinsic pathway and the extrinsic pathway (Figure 2). Apoptosis is mediated by multi-protein complexes called cysteine aspartyl-specific protease (caspases) (Logue & Martin 2008; Nair *et al.* 2014). The intrinsic pathway, which is also known as the mitochondrial pathway, can be activated by various stimuli, including cellular stress, viral infections, toxins, free radicals, or radiation. Damage to the cellular DNA can also induce the activation of the intrinsic pathway (Baig *et al.* 2016; Khan *et al.* 2014).

Mitochondria release cytochrome c, which binds to and activate Apaf-1. Activated Apaf-1 binds to procaspase-9 to form the apoptosome complex. The apoptosome cleaves and activates caspase-9, which leads to activation of caspase 3 and the caspase cascade (Langlais *et al.* 2015; Reubold & Eschenburg 2012).

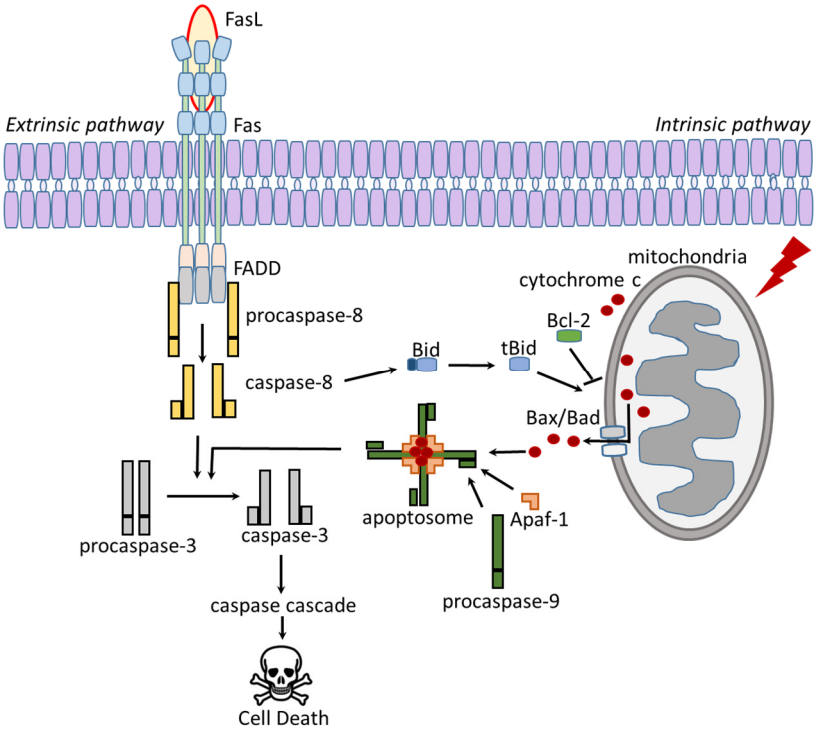

Figure 2. Schematic overview over the apoptotic pathways. Modified from (Sessler et al. 2013).

The extrinsic pathway, also known as the death receptor pathway, can be induced through the activation of death receptors such as Fas (known as CD95) and the tumor necrosis factor receptor (TNFR) (Ashkenazi 2015; Tchikov *et al.* 2011). Binding of the Fas ligand (FasL) induces Fas trimerization, and the Fas trimer recruits the initiator procaspase-8 via the FAS associated death domain (FADD) containing protein. Activated caspase-8 can directly activate caspase-3 which leads to cell death (Fulda & Debatin 2006; Galluzzi *et al.* 2012a; Kaufmann *et al.* 2012).

Apoptosis is expressly regulated by the Bcl-2 protein family. The Bcl-2 family functions both as pro-apoptotic and anti-apoptotic proteins. *Bid* is cleaved and activated by caspase-8, which activate the pro-apoptotic Bcl-2 proteins *Bax* and *Bad* to form mega channels in mitochondrial membranes for cytochrome c release (Goldar *et al.* 2015; Westphal *et al.* 2011). Anti-apoptotic Bcl-2 proteins, such as Bcl-2 itself and Bcl-X_L inhibit *Bax/Bad* activation leading to inhibition of cytochrome c release (Kvansakul & Hinds 2013; Sessler *et al.* 2013).

In contrast to apoptosis, necrosis is cell death in living tissue characterized by cytoplasmic swelling that induce an inflammatory response (Kroemer *et al.* 2009). Specific morphological features, in particular volume changes, accompany cell death processes and are often used to define the different cell death pathways (Krysko *et al.* 2008). A regulated necrotic pathway, also known as necroptosis, is necessary for non-apoptotic signaling and is occurs when caspase-8 is inactive or inhibited. Receptor interacting proteins will instead be activated by FADD (Ouyang *et al.* 2012) and interact with other proteins to form a necrosome complex (Pasparakis & Vandenabeele 2015). Necrosomes stimulate regulated necrosis by activating other proteins followed by necroptosis, and by promoting mitochondrial fragmentation (Galluzzi *et al.* 2012b; Pasparakis & Vandenabeele 2015).

B cell development

Hematopoietic stem cells are produced in the bone marrow and have the unique ability to give rise to all of the different blood cell types and tissues (Wilkinson & Göttgens 2013). Normal B cells express the antigen receptor (BCR) on the surface, which binds antigens and transmits signals that regulate B cell activation, growth and differentiation. The B cell differentiation is a tightly regulated process starting in the bone marrow from a lymphoid stem cell progenitor, the (pro)-B cell (Melchers 2015). In a pro-B cell (Figure 3), the immunoglobulin (Ig) heavy chain genes start to rearrange and when the heavy chain is expressed, the pro-B cell develop to a precursor (pre)-B cell (LeBien & Tedder 2008). The pre-B cell continue the development and rearrange the Ig light chain genes expressing a functional membrane-bound IgM and will then be classified as an immature B cell in the developmental stage. Immature B cells enter a checkpoint, where autoantigens are presented. B cells expressing high-affinity autoreactive BCRs are deleted via a mechanism called negative selection (Köhler *et al.* 2008; Victora & Nussenzweig 2012). B cells expressing low-affinity autoreactive BCRs are positively selected to exit the bone marrow and migrate to the secondary lymphoid organs to produce mature B cells that are characterized by the co-expression of IgM and IgD on the surface together with two signal proteins, Ig- and Ig- heterodimers (Dylke *et al.* 2007; Reth & Nielsen 2014).

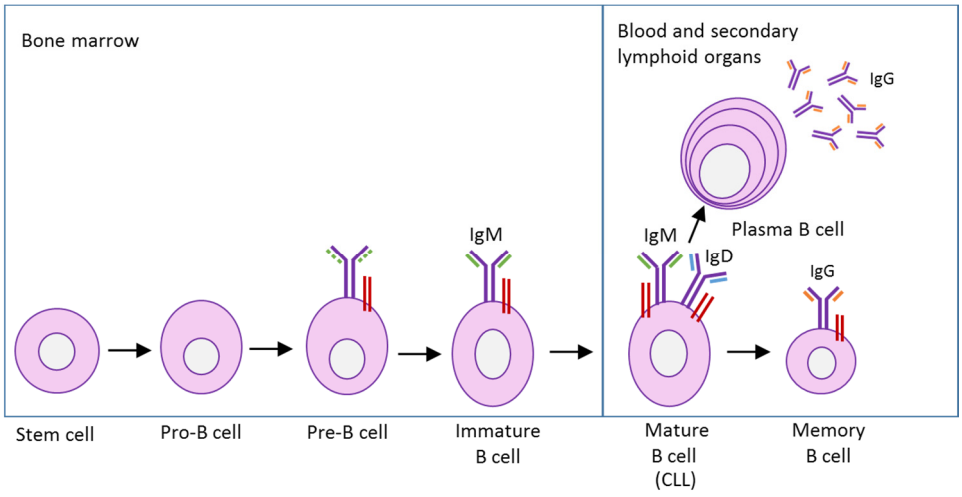

Figure 3. Stages of B cell development.

Normally the body produces autoreactive B cells at high frequency in the bone marrow (Cambier *et al.* 2007). Over 85% of the newly formed immature B cells die in the bone marrow, probably as a consequence of the negative selection (Melchers 2015). Autoreactive B cells must be silenced to prevent autoimmune disease (Nemazee 2006). The silencing occurs by the tolerance mechanisms, clonal deletion, receptor editing and anergy (Figure 4) (Rosenspire & Chen 2015; Yarkoni *et al.* 2010). Clonal deletion is induced cell death by apoptosis. Receptor editing is when the B cell undergoes a second rearrangement forming a receptor specificity for a non-self-antigen instead of the self-antigen (Halverson *et al.* 2004). Finally, anergy is when B cells become tolerant to autoantigens. Anergy can be defined as the functional long term inactivation of autoreactive B cells to further signals through the BCR and it occurs normally when the B cell expresses low affinity for the self-antigen (Hippen *et al.* 2005; Phan *et al.* 2003).

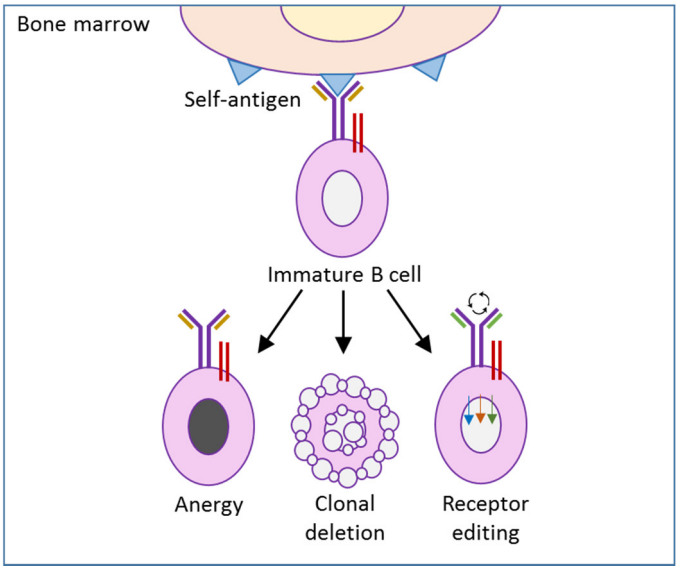

Figure 4. Autoreactive B cell tolerance.

The B cells have to bind to their specific antigen to become activated and start to proliferate when the activating signals are provided from either the T helper cells or when the B cell binds to an antigen via its BCR (Buchner & Muschen

2014; Cerutti *et al.* 2011). Germinal centers are structures in the lymphoid organs where the mature B cells proliferate and class switches take place (Eibel *et al.* 2014; Klein & Dalla-Favera 2008). B cells can change their BCR isotype form to IgG, IgE or IgA, depending on the provided signal (Lanasa & Weinberg 2011; Pieper *et al.* 2013). In the germinal center, the B cells will undergo another checkpoint and cells expressing BCRs with high affinity against the activating antigen will be selected and differentiated into plasma cells or IgG expressing memory B cells. Plasma cells can survive for extended periods of time without cell proliferation (Tokoyoda *et al.* 2009; Tokoyoda *et al.* 2010).

Leukemia and lymphoma

During development of hematopoiesis, different disruptions of cell division, differentiation and apoptosis may lead to mutations and disorders that can case leukemia or lymphoma (Packham *et al.* 2014). Leukemia and lymphoma are the classifications of tumors of the blood, bone marrow or lymphoid system. Leukemia's are single cells proliferating in the blood or lymph and lymphomas are tumors in the lymphoid tissues proliferating as solid tumors (Goldsby *et al.* 2000). There are different subtypes of leukemia and lymphomas (Jaffe 2009). Examples of the leukemia types include acute lymphoblastic leukemia (ALL); acute myeloid leukemia (AML), chronic lymphocytic leukemia (CLL) and chronic myeloid leukemia (CML). Examples of the lymphomas types include diffuse large B cell lymphoma (DLBCL), follicular lymphoma (FL) and mantle cell lymphoma (MCL) (Jaffe 2001).

Chronic Lymphocytic Leukemia

CLL is the most common hematological malignancy amongst adults in the Western countries. In Sweden, about 400 people are diagnosed with CLL yearly, according to the Swedish Cancer Society, and the median age at diagnosis is 72 years (Baliakas *et al.* 2015).

CLL is characterized by a clonal expansion of neoplastic $CD5^+$, $CD19^+$ and $CD23^+$ B-cells in the peripheral blood (PB), bone marrow (BM), lymph nodes (LN) and spleen (Chiorazzi *et al.* 2005; Hallek *et al.* 2008; Rozman & Montserrat 1995). CLL cells with unmutated Ig heavy chain variable (IGHV) genes are associated with high cell proliferation and a more aggressive form of disease, compared to CLL cells with mutated IGHV genes (Rosenwald *et al.* 2001). Patients with unmutated Ig genes have a median survival of 8 years (Hamblin 2011), while those with mutated Ig genes have an indolent disease with up to more than 25 years survival (Dighiero & Binet 2000; Siddon *et al.* 2013). Herishanu *et al.* showed that CLL cells proliferate highly in the BM and the LN compared to CLL cells in PB, and genes significant for BCR signaling are upregulated in the BM and the LN CLL cells, compared with circulating PB cells (Herishanu *et al.* 2011).

Protein Tyrosine Phosphatases and Kinases

Protein tyrosine phosphorylation is a key mechanism regulating cell signaling and occurs in every physiological process (Alonso *et al.* 2004). Protein tyrosine phosphorylation controls different signaling pathways, and will affect cell proliferation, differentiation and apoptosis as well as cell activation, motility and morphology (Mustelin *et al.* 2005).

The protein tyrosine phosphatase (PTP) SH2-domain containing phosphatase 1 (SHP-1) is a non-receptor tyrosine phosphatase located in the cytoplasm. SHP-1 is a key regulator that controls the intracellular phosphotyrosine level in lymphocytes (Wu *et al.* 2003). SHP-1 acts as a negative regulator of cell signaling in several hematopoietic cells and epithelial cells (Neel *et al.* 2003). SHP-1 mRNA levels are shown to be decreased in lymphoma and leukemia cell lines and tissue, and therefore SHP-1 is proposed to function as a tumor suppressor gene (Amin *et al.* 2007; Khoury *et al.* 2004; Koyama *et al.* 2003; Oka *et al.* 2001).

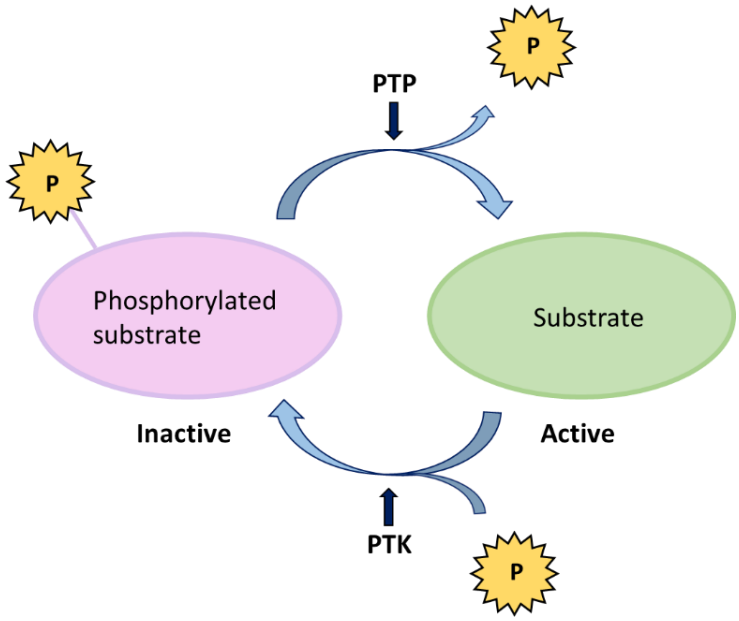

Figure 5. PTP dephosphorylate the tyrosine residues while PTK phosphorylate the tyrosine residues in target substrates. Modified from (Tonks 2013).

Protein tyrosine kinases (PTKs) are enzymes that specifically activate proteins by phosphorylation (Figure 5) and play a key role in cell development and lymphocyte activation (Chakraborty & Weiss 2014). Abnormal PTK expression or activity can lead to malignant transformation and tumor development (Blume-Jensen & Hunter 2001). Figure 6 shows a schematic overview of the BCR and the different proteins involved in the phosphorylation and dephosphorylation of the receptor. SHP-1 is the substrate for various PTKs, such as the Lck/Yes novel protein tyrosine kinase (LYN), Spleen tyrosine kinase (SYK) and the 70 kDa zeta chain associated protein kinase (ZAP70) (Brockdorff *et al.* 1999; Neel *et al.* 2003; Poole & Jones 2005); the PTKs function as suppressors of BCR activation and downregulate the cell proliferation, for example by activation of SHP-1 *(Neel et al. 2003).*

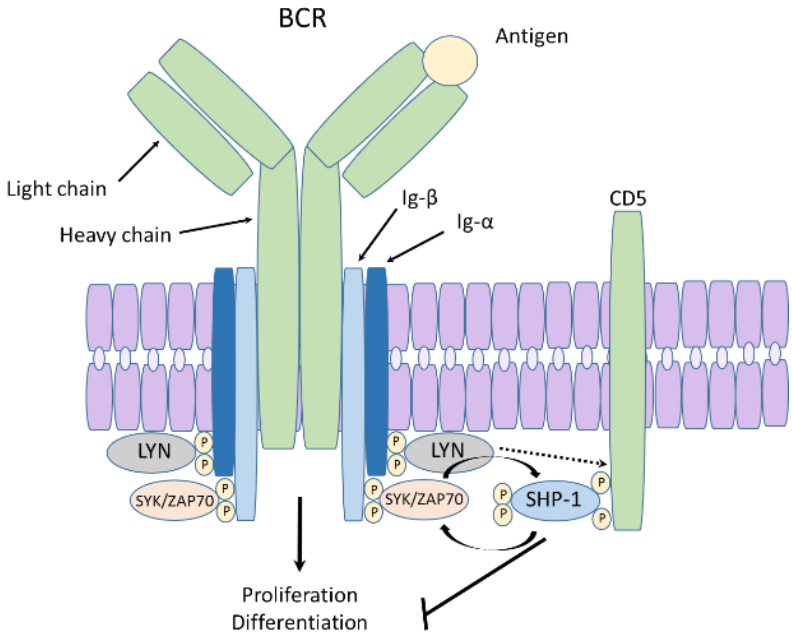

Figure 6. Schematic overview of the SHP-1 activation in CLL. The BCR is activated by binding of the antigen and LYN and SYK phosphorylate the transmembrane proteins Ig-α and Ig-β. LYN phosphorylates CD5 that in turn work as a docking site for SHP-1.

ZAP70 is normally expressed in T cells, thymocytes and natural killer (NK) cells. ZAP70 is overexpressed in CLL cells and ZAP70 positive cells with unmutated Ig genes are correlated with aggressiveness of the disease (Sivina *et al.* 2011; Wiestner *et al.* 2003). The SHP-1 protein has a central role in normal cell growth by regulating the activity of PTKs (Delfani & Wingren 2012), and is similarly expressed in CLL PB cells and normal B cells (Negro *et al.* 2012). In CLL, LYN phosphorylates CD5, which in turn serves as a docking site for SHP-1. When recruited to the plasma membrane, SHP-1 is phosphorylated (Tibaldi *et al.* 2011).

CLL is known to be unresponsive to BCR stimulation because of anergy (Mockridge *et al.* 2007; Muzio *et al.* 2008). Anergized B cells are characterized by a lower sIgM and sIgD expression compared to normal mature B cells (Apollonio *et al.* 2013; Quach *et al.* 2011; Slupsky 2014). CLL with mutated Ig genes (Guarini *et al.* 2008; Herve *et al.* 2005) and with low expression or absence of ZAP70 are correlated with anergy and with unresponsiveness to BCR stimulation (Chen *et al.* 2002; Packham *et al.* 2014). Anergic CLL cells are difficult to treat through BCR signaling pathways. However, the new treatments specifically targeting the BCR signaling pathways are showing promising results on the aggressive form of the CLL and may lead to successful treatment (Friedberg *et al.* 2010; Hoellenriegel *et al.* 2011; Ponader *et al.* 2012).

Treatment

Patients with CLL have longer survival rates due to the large number of promising new therapeutic agents and cellular therapies (Mato *et al.* 2015). New biological markers and improved prognosis may allow for a more targeted individualized therapy (Vaque *et al.* 2014). CLL is an indolent disease that has a highly variable clinical course. Two prognostic staging systems exist, the Rai classification (Rai *et al.* 1975) and the Binet classification (Binet *et al.* 1981). One of the main challenges in cancer treatment today is to choose the proper individual treatment for each cancer patient. The three main treatment strategies presently used are chemotherapy, targeted therapy, and monoclonal antibody therapy. When the patient does not show any symptoms, normally the "watch and wait" policy is used and in those cases no treatment is needed (Else *et al.* 2008).

Molecular Imprinting Polymers

Glycans are polysaccharides that are present on the surface of all cells. Glycans are involved in cellular communication and in processes such as cell differentiation, proliferation and infection, including protecting the cells from invaders and in cell-cell contacts (Adamczyk *et al.* 2012; Varki & Lowe 2009). Sialic acid (SA) is a monosaccharide, terminally expressed at the end of glycan chains, which functions as a cell marker, and can be recognized by a variety of receptors (Ohtsubo & Marth 2006). SA plays an important role in immunity regulation and may have an inhibitory effect on immune activation (Fujita *et al.* 1999). The two main common forms of SA in nature are human *N-Acetylneuraminic* acid (Neu5Ac) and nonhuman *N-glycolylneuraminic* acid (Neu5Gc). Nonhuman Neu5Gc has been found in normal human cells, where it has been absorbed from the food intake, especially from red meat (Samraj *et al.* 2014; Tangvoranuntakul *et al.* 2003).

In the late 1980s, researchers started to realize an association between SA and cancer, especially in metastatic cancer (Dennis *et al.* 1989; Hoff *et al.* 1989). The SA expression is increased in metastatic cancer cells (Cui *et al.* 2011; Varki & Varki 2002) and overexpression is reported to affect tumor cell growth and cell differentiation (Ferreira *et al.* 2013; Seidenfaden *et al.* 2003).

A common detection method for analyzing glycans is using labelled lectins (Cho *et al.* 2014). The availability of specific antibodies against SA is limited due to difficulties to discriminate between various glycan species in combination with low specificity and affinity to SA (Cummings 2009; Fujitani *et al.* 2013). Molecular imprinting polymers (MIP) is a technique to design selective artificial receptors produced by allowing a polymer to form in presence of a template. After removing the template, the resulting MIP can be used as a plastic antibody (Vasapollo *et al.* 2011). Recently, different monosaccharide imprinting procedures have been used to produce fluorescently labeled probe nanoparticles displaying an unprecedented affinity for the targeted terminal monosaccharides in cell staining experiments (Kunath *et al.* 2015). Based on a ternary complex imprinting approach we developed SA-imprinted core-shell nanoparticles, conjugated with a fluorescent reporter group (Shinde *et al.* 2015); the SA-MIP binds specifically to SA on the cell surface (Figure 7). The main advantage of this technique is that it displays a high affinity and selectivity for SA (Alexander *et al.* 2006) and have high stability compared to antibodies (Whitcombe *et al.*

2011). We have recently shown that SA-MIPs selectively targeted prostate cancer and leukemia cell lines, using flow cytometry and fluorescence microscopy (Shinde *et al.* 2015).

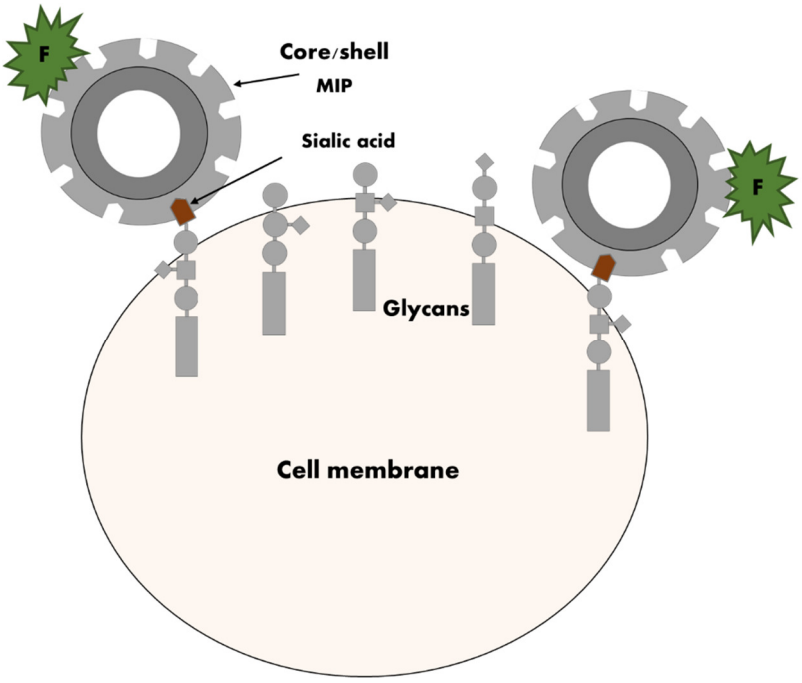

Figure 7. Principle of using MIPs as "plastic antibodies" for imaging of sialic acid terminated glycan motifs. Modified from (Shinde et al. 2015).

Digital Holographic Microscopy

Dennis Gabor discovered the fundamentals of holography in the late 1940s and in 1971 he received the Nobel Prize in Physics for this development (Gabor 1949). Since then, holography has become a well-established imaging technique. Digital holographic (DH) microscopy is a digital high resolution holographic imaging technique with the capacity of quantification of cellular conditions without any staining or labeling of cells (Alm *et al.* 2011; Marquet *et al.* 2005; Rappaz *et al.* 2005).

DH microscopy builds on red coherent laser light, from a diode laser. The primary light beam is split into two beams, an object beam and a reference beam. The object beam will pass through the sample, which in this case are living cells, and then merge with the reference beam, thus creating an interference pattern (Figure 8). The interference pattern will be captured by a light detector (*e.g.*, a CCD-sensor) and computer algorithms convert the signal into a holographic image based on the light phase shifting properties of the cells (Xiao & Puri 2002). The three-dimensional holographic image is then an impression of the real cells (Sebesta & Gustafsson 2005).

Various cellular parameters can be visualized and calculated from the particular hologram, including the area, thickness, volume, confluence, and the number of cells (Carl *et al.* 2004; Chalut *et al.* 2012; Ferraro *et al.* 2005; Kemper *et al.* 2006; Lenart *et al.* 2008; Mann *et al.* 2005). Traditional fluorescence and light microscopy may cause phototoxicity, and therefore researchers have attempted to develop non-damaging microscopy methods (Frigault *et al.* 2009; Hoebe *et al.* 2007). As only very low light intensity is needed, the DH technique is a non-destructive and non-phototoxic method (Logg *et al.* 2009) allowing for both qualitative and quantitative measurements of living cells (Yu *et al.* 2009).

DH microscopy has been used to study different cell types e.g. protozoa, bacteria, and plant cells. Mammalian cells such as nerve cells, stem cells, various tumor cells, bacterial-cell interactions, red blood cells, and sperm cells have also been investigated (Alm *et al.* 2013). The first DH microscopy images showing living cells were published in 2003, making this a rather new research field (Yu *et al.* 2003).

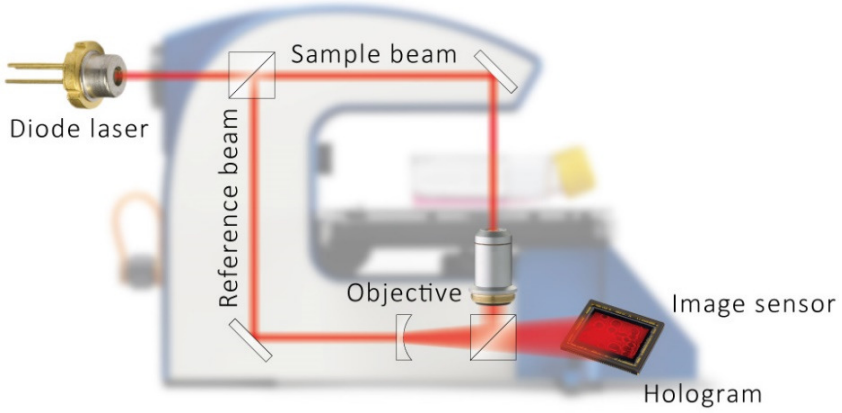

Figure 8. Schematic view of the DH microscopy technique (www.phiab.se).

Using DH for counting the number of cells and estimating the confluence directly in the culture vessels is very useful. Moreover, cell viability status can be determined using DH microscopy (Kemmler *et al.* 2007). One large benefit of DH is the ability to differentiate between viable and non-viable cells without any laborious and time-consuming staining or labelling of the cells with common dyes, such as trypan blue or propidium iodide (Khmaladze *et al.* 2012; Mölder *et al.* 2008).

DH microscopy can be compared to other techniques such as electronic cell sizing and atomic force microscopy for detection of differences of volumes in cell death induced human epithelial cells. The different methods give comparable results, but DH was shown to be advantageous due to noninvasive labeling, the time resolution, and allowing measurements of both single cells and populations (Khmaladze *et al.* 2012).

Several studies have demonstrated changes in cell volume for cell death analysis using DH. The interest for analyzing cell volume changes with DH microscopy, resulting from cytotoxic events or apoptosis treatment has recently increased in popularity (Alm *et al.* 2013; Kühn *et al.* 2013; Pavillon *et al.* 2012; Trulsson *et al.* 2011; Wang *et al.* 2013). When cells go in to early apoptosis, the first discernable indication is a decrease of the cell phase shift. Pavillion *et al.* recognized

early apoptotic cells within minutes by their DH phase signal, while it took several hours to identify dead cells using trypan blue staining.

Cell cycle control plays an essential role in cell differentiation and proliferation. Several proteins, mainly cyclins and cyclin dependent kinases (CDKs) in the checkpoints of the cell cycle stringently control cell proliferation. (Coleman *et al.* 2004). Mutations in regulating proteins such as cyclins and CDKs result in uncontrolled cell proliferation leading to development of cancer (Malumbres & Barbacid 2001). DH can identify specific changes in cell volume that correlate to either G1 or G2/M arrest. Average cell volume changes in response to treatment with cell cycle arresting compounds could therefore be used as a DH marker for monitoring cycle arrest in cultured cells. Interestingly, the results showed comparable accuracy to flow cytometry measurement of cell cycle phase distribution (Miniotis *et al.* 2014).

DH can recognize small morphological changes between different cell types, treated with the same cytotoxic drugs. Alm *et al.* have presented results from individual cells where a prostate cancer cell line and a mouse fibroblast cell line were treated with a cell death inducing drug. The prostate cancer cell line contracted, became dense and rounded up over time and the cell fragmented (Figure 9). The mouse fibroblast cell line behaved very differently, with some cells starting to die within one hour and others after several hours after treatment; the cells became thinner and thinner and eventually disappeared, *i.e.*, necrosis (Alm *et al.* 2013). In addition, Colomb *et al* showed details of the apoptotic process, where the apoptotic blebbing in prostate cells was clearly visualized by DH microscopy (Colomb *et al.* 2008).

DH microscopy is mainly used for adherent cells. Suspension cells are difficult to analyze using DH microscopy since they are floating at several different levels in the medium. To facilitate DH microscopy analysis of death-induced suspension cells, we have introduced antibody-based microarrays (Wingren *et al.* 2009) to the experimental DH set-up. By using single-chain variable antibody fragments (scFv), (Borrebaeck & Wingren 2011) directed against some of the most common cell membrane proteins on T- and B-lymphocytes, suspension cells can be analyzed.

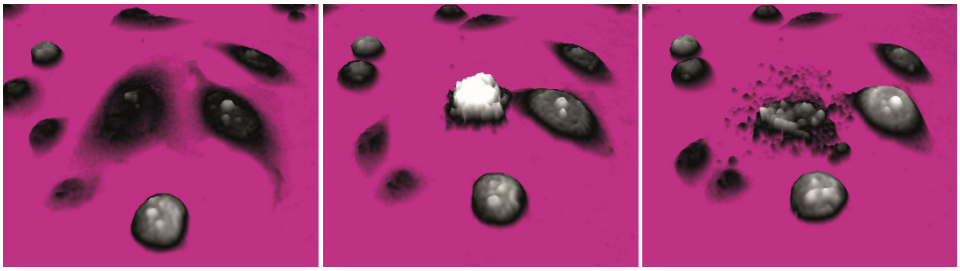

Figure 9. 3D holographic images showing a dying cancer cell (www.phiab.se).

Antibody microarrays are used today for multiple screening of biomarkers in different diseases (Wingren *et al.* 2009). Recombinant antibody microarrays have been developed for cell surface membrane proteomics for immunophenotyping by using different scFv (Dexlin *et al.* 2007) and they were tested to work well in microarray applications (Dexlin-Mellby *et al.* 2010; Dexlin-Mellby *et al.* 2011). Stybayeva et al used CD4/CD8 antibody specific microarrays combined with two-dimensional lensfree holographic imaging by first capture the cells on CD4/CD8 scFv coated slides and then detecting the cytokine signals by cytokine immunoassay (Stybayeva *et al.* 2010).

Antibody-based microarray techniques have been used to determine phenotypic protein expression profiles for human B cell sub-populations (Ellmark *et al.* 2008). Antibody-based microarrays have also been used to detect soluble antigens (Belov *et al.* 2006). Antibody-based microarrays enable screening of live suspension cells for the expression of large numbers of cell surface CD antigens. Such profiling classify the CD antigens for leukemia classification and drug target identification (Barber *et al.* 2009; Kohnke *et al.* 2009). Figure 10 is a 3D hologram image showing captured cells on an antibody microarray.

DH microscopy makes it possible to analyze cells without affecting them in any way. The unique measurable parameters are the cell number, cell area, thickness, and volume, which can be coupled to proliferation, migration, viability and cell death. Cell morphology parameters can be very useful when following the effects of different treatments, the process of cell viability, as well as growth and cell death. The technique is cheap, fast and simple to use and have unique

imaging capabilities for time-lapse investigations both on the single cell- and the cell-population levels.

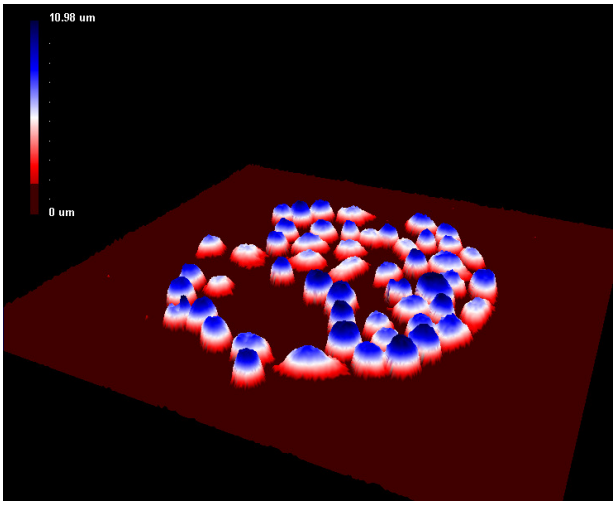

Figure 10. Antibody-based microarray combined with DH microscopy. Jurkat cells captured on antibody Lewis X (El-Schich Z.).

AIMS OF THE THESIS

Paper I

To study SHP-1 expression and activity in chronic lymphocytic leukemia patients using matched lymph nodes and peripheral blood samples.

Paper II

To analyze sialic acid expression on leukemic cells by using sialic acid molecular imprinted polymerase.

Paper III

To investigate whether death-induced cancer cells can be distinguished from untreated cells by the use of digital holographic microscopy.

Paper IV

To develop digital holography for cell death analysis of suspension cells by combining digital holographic microscopy with antibody-based microarrays.

METHODS

Patient samples

(Paper I)

Mononuclear cells from patients diagnosed with CLL from PB and LN were isolated by Ficoll gradient centrifugation. CLL cells were purified by negative selection with B-CLL cell isolation kit (Miltenyi Biotec). The purity of the selected B-CLL cells were approximately 97% as assessed by flow cytometry using CD5/CD19 antibodies. The selected CLL PB cells were cultured and BCR stimulated with anti-IgM (Thermo Fisher Scientific) for 10 minutes, 30 minutes or 48 hours or left unstimulated as a negative control. BCR stimulated and unstimulated cells were then used for flow cytometric analysis and Western blot analysis as described below.

Ethics

(Paper I)

Informed consent was obtained from all CLL patients according to the Declaration of Helsinki, and ethical approval was granted by the ethical review committee at Linköping University.

Cell lines

(Paper II-IV)

Several different cell lines were used depending on the topic of the investigation. In paper II, four human CLL cell lines were used. HG3, CI, Wa-osel and AIII were from the Department of Clinical and Experimental Medicine, Linköping, Sweden. The mouse fibroblast cell line L929 and the human prostate cancer cell line DU145 were obtained from The American Type Culture Collection (ATCC) and used in paper III. In paper IV, two selected cell lines were used: the human diffuse large B cell lymphoma cell line U2932 obtained from the Department of Oncology, Genetics and Pathology, Uppsala, Sweden, and the T cell acute lymphoblastic leukemia cell line Jurkat, obtained from ATCC.

Quantitative PCR

(Paper I)

The RNA expression was evaluated using quantitative PCR (q-PCR). Total RNA was isolated from purified CLL cells from matched PB and LN patient samples using the Allprep DNA/RNA mini kit (Qiagen). The synthesis of cDNA was performed using the Verso cDNA kit (Thermo Fisher Scientific). The mRNA expression levels for *SHP-1* and *Ki-67* were quantified using q-PCR analysis with SYBR Green probes (Roche). The samples were analyzed and run on a Light Cycler 480 II real time PCR system (Roche) and normalized against a reference gene (*GAPDH*).

Western blot analysis

(Paper I)

To determine the expression of SHP-1 and phosphorylated SHP-1, western blot analyses were performed. The selected CLL PB cells and cells from matched PB and LN were lysed at 4 °C in ice-cold lysis buffer supplemented with protease inhibitors (Roche) and phosphatase inhibitors. The cell lysates were collected and cleared by centrifugation at 15,000 g. All samples were normalized to ensure equal loading. Protein extracts were denatured at 65 °C in sample buffer and, separated by SDS-PAGE (Bio-Rad). The separated proteins were transferred to a PVDF membrane, and blocked overnight in Tris-buffered saline (TBS) containing 0.1 % Tween-20 and 5 % BSA. The membranes were incubated with the following antibodies: anti-SHP-1 (Santa Cruz), anti-phospho-SHP-1 Y536, phospho-SHP-1 S591 (Abcam) or -actin (Dako). After three washes with TBS containing 0.1 % Tween-20 and 5 % BSA, the membranes were incubated with HRP-conjugated secondary antibodies (Dako). Immunodetection and quantification was performed on an enhanced chemiluminescence detection kit on a ChemiDocMP Imaging system (Bio-Rad).

Immunoprecipitation and protein tyrosine phosphatase assay

(Paper I)

In order to measure the activity of SHP-1, cell lysates of matched PB and LN cells were incubated with anti-SHP-1 antibody conjugated to agarose beads (R&D systems) and incubated for 3 hours with constant rotation. The beads were then washed two times with lysis buffer and once with reaction buffer. Tyrosine phosphatase substrate I was added and incubated for 30 minutes at 37°C with constant rotation. After incubation, the samples were transferred to

a microplate and the reaction was terminated by adding Malachite Green Reagent A and incubated for 10 minutes at room temperature (RT) and thereafter Malachite green reagent B was added and incubated for 20 minutes more at RT. The absorbance was measured at 620 nm using BIO-TEK® microplate reader and the results were compared with a phosphate standard.

Flow cytometry analysis

(Paper I-II)

To investigate the expression level of SHP-1, intracellular flow cytometric analysis was performed (Paper I). The selected CLL cells from anti-IgM stimulated or unstimulated PB cells and cells from matched PB and LN samples, were fixed in 4% paraformaldehyde, permeabilized with 0,05% saponin, and incubated with anti-SHP1-PE (Santa Cruz). The cells were analyzed using an Accuri C6 Flow Cytometer (BD Biosciences).

The surface expression of SA was investigated by flow cytometry (Paper II). The cells were fixed with 4% formaldehyde and incubated with sonicated SA-MIP or left in 3 % methanol/water as a negative control. The cells were incubated at 37 °C with 5% CO_2, for 60 minutes. For analyzing the expression level of the glycans, the cells were incubated with lectin-FITC or left unstained as a negative control and incubated in darkness on ice for 20 minutes. The cells were analyzed using flow cytometry.

Fluorescence microscopy

(Paper II)

To analyze the binding of SA on cancer cells, fluorescence microscopy was used. Cells were adhered to polylysine treated slides for two hours, at 37 °C with 5% CO_2 at 100% humidity. After incubation, the cells were fixed with 4% formaldehyde and incubated with sonicated SA-MIP or left in 3 % methanol/water. The cells were incubated at 37 °C with 5% CO_2, for 60 minutes. After incubation, the cells were washed and incubated with DAPI (Thermo Fisher Scientific) for 4 minutes at RT for nuclear staining. The cells were mounted with one drop of mounting medium reagent (Molecular probe) and analyzed using fluorescence microscopy (EVO® LS 10, Carl Zeiss).

In order to analyze the expression level of the glycans, lectin-FITC was used. Cells were grown on polylysine treated slides for two hours, at 37 °C with 5%

CO_2 at 100% humidity. After incubation, the cells were fixed with 4% formaldehyde and incubated with lectin-FITC in PBS, or left unstained as a negative control. The cells were incubated at RT for 60 minutes. After incubation, the cells were washed and incubated with DAPI for 4 minutes at RT for nuclear staining. The cells were mounted with one drop of mounting medium reagent and analyzed using fluorescence microscopy.

Reagents

(Paper III-IV)

Etoposide was dissolved in dimethyl sulfoxide (DMSO, Sigma– Aldrich) to investigate the cell death response. Etoposide was used at final concentrations of 1, 5 and 10 μM for up to 3 days (paper III). To obtain a cellular response (paper IV), etoposide was used at a final concentration of 500 μM for up to 16 hours.

Cell viability measurements

(Paper III)

To measure cell viability using DH microscopy, different concentrations of cells were seeded into 25 cm^2 flasks and allowed to adhere for 24 hours. The cells were incubated further for 24, 48, 72 and 96 hours. Cell growth was monitored with DH microscopy and several images were captured from each sample over time and analyzed as described below.

In order to measure cell viability after etoposide treatment, cells were seeded into 96-well plates and allowed to adhere for 24 hours followed by etoposide treatment for 24, 48, 72 and 96 hours. MTS-assays were performed by adding MTS solution (Promega) to the wells and the cells were then incubated for 2 hours. The absorbance was measured at 490 nm using a BIO-TEK® microplate reader. The MTS assay is a colorimetric method for sensitive quantification of viable cells and is based on reduction of the MTS solution by the cells, to generate a colored product.

Antibody-based microarrays

(Paper IV)

For detection of captured cells, recombinant antibody arrays containing different surface scFv were immobilized on glass slides through passive adsorption. Suspension cell lines were left to bind for 30 minutes on the antibody-based microarrays. After the incubation, attached cells were washed and treated with

either etoposide, DMSO, or left untreated as a negative control. By using DH microscopy, morphologic changes due to cell death were captured and analyzed as described below.

DH microscopy analysis

(Paper III-IV)

To detect morphology changes of death-induced cells, DH microscopy was used. The cells were treated with etoposide and incubated for up to 3 days and each day DH microscopy images were acquired. Several images were captured from the samples over time and data of the cell number, confluence, cell volume, and cell area were obtained (paper III).

Time-lapse series were run for 16 hours (paper IV). Holographic imaging was performed every tenth minute for the same cell population. Image areas covered with cells were then segmented using an automated computer algorithm *Hstudio*, obtaining data of the cell number, confluence, area, volume, thickness, eccentricity and irregularity.

Statistical analysis

(Paper I and III)

Mean and standard deviation were calculated for statistical analysis in paper I and III. For the q-PCR results p-values were calculated. For the cell viability and cell death studies, at least 20 images per sample were captured from at least two independent experiments.

RESULTS AND DISCUSSION

BCR signaling suppressor SHP-1 is active in CLL lymph node and peripheral blood (Paper I)

SHP-1 expression and activity is downregulated or lost in several leukemias and lymphomas (Amin *et al.* 2007; Khoury *et al.* 2004). This suggests that loss of SHP-1 expression might be associated with both malignant transformation and tumor cell aggressiveness (Kossev *et al.* 2001; Wu *et al.* 2003). In the present study, we hypothesized that SHP-1 would be downregulated or inactivated in the proliferative center, the LN cells. Considering that SHP-1 is a key phosphatase for suppression of BCR signaling, we analyzed the SHP-1 expression and function in CLL proliferative LN cells in comparison with the PB cells. We found that SHP-1 gene expression was decreased in 50% of patients in proliferating LN cells when compared to PB cells of the same patient. Interestingly, the expression of the proliferative *Ki-67* gene expression level in these patient samples was higher in LN than in PB, indicating lower SHP-1 expression in more proliferative cells. However, differences in SHP-1 protein expression could not be detected in LN and PB.

Since higher proliferative activity was seen, we investigated the phosphatase activity of the BCR suppressor SHP-1. The results showed SHP-1 phosphorylation in PB and LN samples. However, no significant differences in SHP-1 phosphorylation comparing PB with LN could be observed. These results of SHP-1 protein and *SHP-1* gene downregulation in LNs *in vivo* may be part of a strategy for anergy maintenance in CLL, or alternatively it may indicate loss of function by mutation (Vollbrecht *et al.* 2015; Weibrecht *et al.* 2007). No changes of SHP-1 phosphorylation after short time BCR stimulation (10 and 30 minutes) of PB cells could be seen, however we observed a significant downregulation of phosphorylated SHP-1 in 48 hours BCR stimulated cells. This is in line with findings in B1 cells in which CD5-SHP-1 association continues upon BCR engagement. This limits the B cell response and B1 cells are retained in the anergic state (Sen *et al.* 1999). This observation is noteworthy, since CLL B cells share several

properties with B1 B cells, including $CD5^+$ expression and the anergic condition (Bergh *et al.* 2014; Rosén *et al.* 2012).

Different expression levels of glycans on leukemic cells - a novel screening method with molecularly imprinted polymers (MIP) targeting sialic acid (Paper II)

The SA expression level is known to be increased in metastatic cancer cells (Ferreira *et al.* 2013; Seidenfaden *et al.* 2003), and hence, it is of importance to analyze and determine the SA expression. However, the task is challenging owing to the limited availability of SA specific antibodies (Cho *et al.* 2014; Fujitani *et al.* 2013). We have recently presented a novel method for specific detection of SA using MIP-technology (Shinde *et al.* 2015). The aim of this study was to perform an extended screening of SA expression by using SA-MIPs, including four different CLL cell lines, conveniently analyzed by flow cytometry and fluorescence microscopy.

Our results showed that SA is expressed in the plasma membrane in all four CLL cell lines at different levels. A higher expression of SA in the more aggressive CLL cell lines was observed. HG3 and CI showed a higher expression compared to the cell lines Wa-osel and AIII. Lectin binding confirmed the results in the CLL cell lines, and HG3 and CI displayed increased lectin binding, compared to the cell lines Wa-osel and AIII. This is in line with the fact that the aggressiveness of the cancer cells correlates with increasing SA levels (Cui *et al.* 2011; Wang *et al.* 2009). HG3 and CI have unmutated IGHV genes, which are associated with high cell proliferation and a more aggressive form of CLL. This is in comparison to Wa-osel and AIII cells, which have mutated IGHV genes, a signature for less aggressive CLL cells (Rosenwald *et al.* 2001).

In order to evaluate the SA-MIP binding to the plasma membrane of the CLL cell line HG3, cells were stained with SA-MIP or lectin-FITC and analyzed using fluorescence microscopy. Overall, the SA-MIP led to a plasma membrane staining of the cells in a similar way as did the lectin.

These results showed that SA-MIP can be used as a plastic antibody for detection of SA using both flow cytometry and fluorescence microscopy. We suggest that SA-MIPs can be used for screening of different circulating tumor cells of

various stages, including CLL cells. Further analysis of the SA expression should include primary CLL cells from patient samples.

Induction of morphological changes in death-induced cancer cells monitored by holographic microscopy (Paper III)

DH microscopy is an approach for label-free non-invasive imaging of cultured cells, in order to monitor growth, viability, and death (Kemper *et al.* 2010; Yu *et al.* 2009). The aim of this study was to investigate whether death-induced cancer cells can be distinguished from untreated cells using DH microscopy. In the present study, we have investigated the morphological changes in two cell lines using DH microscopy. We used a strategy similar to a previous study, aiming at counting cells (Mölder *et al.* 2008). L929 and DU145 cells were treated with different concentrations of etoposide and incubated over time. This analysis was confirmed by a MTS assay.

The number of control cells increased over time, while for treated cells, the numbers of cells was unchanged over time for L929 and DU145. The confluence decreased for treated L929 cells compared to control cells that showed an increased confluence over time. While for treated DU145 cells, the confluence changed depending on the etoposide concentration and time points. However, treated L929 and DU145 cells showed increased cell area and cell volume compared to untreated cells. The hologram images showed morphological changes of etoposide treated L929 and DU145 cells over time compared to untreated cells. The morphological changes were both time and concentration dependent for both cell lines. At the highest concentration Etoposide induced cell death in both cell lines already after 24 hours.

With DH microscopy, small differences between the two cell lines were clarified. L929 showed a lower sensitivity for etoposide at the lowest concentrations, while for DU145 the confluence, cell area, and volume increased at first, and then decreased over time. Our results showed that untreated control cells could be distinguished from etoposide treated cells by determining cell number, confluence, and morphological changes such as cell area and cell volume. Indeed, the use of DH microscopy as a fast, automatic, and cost efficient evaluation tool for different cancer treatments was promising. We believe that DH microscopy is an important tool for personalized medicine investigations, determining the

optimal therapeutic concentration for both individual treatment and for different cancer types.

Interfacing antibody-based microarrays and digital holography enables label-free detection for loss of cell volume (Paper IV)

DH microscopy has mainly been used for adherent cells (Marquet *et al.* 2005). Our previous results in paper III were based on adherent cells. Suspension cells are difficult to analyze using DH microscopy. The aim of this study was to develop DH microscopy for cell death analysis of suspension cells by combined analysis with antibody-based microarrays. Here, we have uniquely introduced antibody-based microarrays (Wingren *et al.* 2009) to the experimental DH setup. The DH microscopy combined with recombinant antibody microarrays provides a totally new capability regarding specific capture of suspension cells. In the present study, we have used DH microscopy for analyzing the cell area, thickness, and volume to evaluate the cell death progression in suspension cell lines.

To investigate the cellular responsiveness, Jurkat and U2932 cells were treated with either etoposide or DMSO and holograms were collected over time. Data for cell number, cell area, cell thickness, cell volume, cell eccentricity, and cell irregularity were collected for both cell types. Untreated Jurkat and U2932 cells showed stable cell numbers over time and the two cell lines showed cell-specific results of cell area and cell irregularity after treatment. The cell volume could be analyzed in cells treated for up to 16 hours, showing a decrease in both cell lines, whereas the volume of untreated cells was unchanged. Interestingly, the U2932 cells showed a slightly different pattern compared with the Jurkat cells. The mean cell area for the U2932 cells was slightly smaller compared with the area of the Jurkat cells. Taken together, we have for the first time shown that that DH microscopy in combination with antibody-based microarrays can be used to analyze treated nonadherent leukemia cells in real time.

Our results provide support for using the concept of DH microscopy combined with antibody-based microarray technology as a novel method for detecting morphological changes in specifically captured death induced cells. Development of fast and accurate evaluation tools for cancer treatments will be of great value to clinicians in deciding the most appropriate treatment for patients.

CONCLUDING REMARKS

The main finding in this thesis are as follows:

Paper I

- 50% of the patient samples showed high *SHP-1* gene expression in PB compared to LN and low *Ki-67* gene expression in PB compared to LN.
- No significant differences in SHP-1 protein expression and SHP-1 phosphatase activity were observed in PB compared to LN.
- We suggest that absence of SHP-1 protein and gene downregulation or activation in proliferative centers/LNs *in vivo* may be part of a strategy for anergy maintenance in CLL, or alternatively it may indicate loss of function.
- A limitation of our study is the low number of available matched LN and PB patient samples. Additional patients are required to elucidate the importance of SHP-1 in CLL pathogenesis.

Paper II

- SA-MIP have high specificity and affinity for SA and can be used as a plastic antibody for detection of SA using both flow cytometry and fluorescence microscopy.
- SA is differentially expressed in CLL cell lines and the expression is correlated to the aggressiveness.

Paper III

- DH microscopy is an excellent tool for cell-death analysis, where decrease of the cell volume could be analyzed in adherent cancer cells.

Paper IV

- The analyzed treated cells showed a decrease in volume, whereas the volume of untreated cells was unchanged.
- Our results offer support for using the concept of DH microscopy combined with antibody-based microarray technology as a novel method for detecting morphological changes in specifically captured death induced cells.

Taken together, this thesis takes cancer research one step further, which could lead to a more individualized treatment for patients and for screening of circulating cancer cells and metastasizing cancer cells in the body.

POPULÄRVETENSKAPLIG SAMMANFATTNING

Cancer är en ledande dödsorsak i världen och är ett samlingsnamn på många olika sjukdomar. Cancer utlöses av att DNA i en cell muteras. Mutationen kan påverka gener som kodar för specifika proteiner, vilka kontrollerar cellen. Cellen blir då okontrollerbar och vissa cancerformer kan metastaseras till andra organ i kroppen. Cancerceller kännetecknas av förmågan att undvika apoptos, det vill säga programmerad celldöd. Apoptos karakteriseras av en mängd olika cellulära morfologiska förändringar. I normala celler är celldöd och celldelning strikt kontrollerat via olika signaleringsvägar, där olika proteiner aktiveras eller inaktiveras beroende på vilken signal cellen får.

I Sverige insjuknar ca 400 människor i kronisk lymfatisk leukemi (KLL) varje år och medianåldern för diagnos är 72 år. KLL påverkar B-celler i kroppen. B-celler producerar antikroppar, vilka angriper främmande organismer som en del av immunförsvaret. KLL cancerceller växer långsamt, vilket gör att de inte alltid slås ut av kemoterapeutiska läkemedel.

Avhandlingen har framför allt fokuserat på biomarkörer och teknikutveckling i cancerforskning för en bättre diagnos och en framtida individuell patientbehandling. Syftet med studie I var att analysera olika signaleringsvägar i KLL som kan förhindra celltillväxten. Vi har analyserat ett protein som heter SHP-1 och som visar högt uttryck i KLL-celler. SHP-1 är en signalmolekyl och har sin normala funktion i cellulära processer, inklusive celltillväxt och differentiering. Vår hypotes är att SHP-1 är högre uttryckt i perifert blod och därmed förhindrar tillväxten av KLL celler, jämfört med lymfknutan. Resultatet visar att hälften av de analyserade patientproverna uttryckte högre SHP-1 i perifert blod jämfört med lymfknutan. Dock kunde vi inte se någon skillnad mellan SHP-1 aktivitet i perifert blod och lymfknutan.

Det är en utmaning för forskare att finna optimal behandling av cancer. Ofta är det svårt att diagnostisera cancer i ett tidigt stadium. Strävan att finna effektiv

teknik och nya biomarkörer för att upptäcka cancer i ett tidigt stadium har varit fokus för forskare i flera år. I studie II har vi undersökt sialinsyra som finns på cellytan. Sialinsyra, som är en del av kolhydratstrukturer, är känd för att vara högt uttryckt i cancerceller och ännu högre i metastaserande celler. Sialinsyra är svår att mäta för att det är svårt att producera antikroppar mot kolhydratstrukturer. Syftet med arbete II var att mäta sialinsyra på cancerceller genom att använda teknologin molekylärt präglade polymerer, MIP. Med hjälp av MIP som binder till sialinsyra har vi lyckats mäta och klassificera sialinsyra i aggressiva KLL-celler jämfört med andra mindre aggressiva KLL-celler. Framtida MIP forskning kan leda till tidig diagnos av cirkulerande cancer celler.

Digital holografi (DH) mikroskopi är ett mikroskop med en inbyggd laser som kan analysera levande celler direkt i odlingskärlen. Man får en 3D-bild av cellerna och uppgifter om olika morfologiska mätvärden som antal celler, celltäthet, area, volym och tjocklek av cellerna i odlingskärlet. Syftet med studie III var att analysera celldöd med hjälp av DH-mikroskopi på behandlade celler. Vi har behandlat två cellinjer med kemoterapeutiska läkemedel och analyserat dem med DH-mikroskopi under flera dagar. Resultaten visar typiska apoptoskaraktärer där volymen, arean och tjockleken minskar och cellerna krymper ihop. Vi har kunnat mäta specifika skillnader mellan cellinjerna som resultat av kemoterapirespons. Framtida forskningsområden kan inkludera patientprover där man snabbt och enkelt kan testa olika behandlingar med DH, för att sedan välja den behandling som patienten svarade bäst på. Detta innebär en möjlighet att skräddarsy cancerbehandling för den enskilde patienten.

DH-mikroskopi har främst använts för celler som växer på ytan i botten av odlingskärl. Det har varit en utmaning att analysera leukemiceller med DH-mikroskopi eftersom leukemiceller flyter runt, vilket gör det svårt att analysera. Syftet med studie IV var att mäta celldöd av leukemiceller med hjälp av DH-mikroskopi kombinerad med en antikroppsbaserad analys. Vi har först fångat upp cellerna med specifika antikroppar som är bundna på en yta och sedan behandlat cellerna med kemoterapi och analyserat med DH-mikroskopi. Resultatet visade att cellerna band specifikt till antikropparna och satt bundna där under hela analysen. Behandlingen med kemoterapi visade typiska apoptoskaraktärer där cellvolymen, arean och tjockleken minskade. Här kunde vi också konstatera olikheter i cellrespons hos de två olika cellinjerna. Det bekräftar våra resultat där behandlingsrespons kan användas för bättre individuell patientbehandling.

Sammanfattningsvis tar denna avhandling ett steg längre inom cancerforskningen, vilket skulle kunna leda till en mer individualiserad behandling för patienter och för diagnos av cirkulerande och metastaserande cancerceller i kroppen.

ACKNOWLEDGMENTS

Jag vill tacka alla som har varit involverade i min avhandling och speciellt tack till min huvudhandledare **Anette**, för att ha introducerat mig till forskningsvärlden redan 2007, och gett mig möjligheten att doktorera på Malmö Högskola. Tack för att du alltid har brytt dig och gett mig all den tid jag behövde. Framför allt tack för ditt tålamod, din vänlighet och omtanke.

Jag vill rikta ett stort tack till mina handledare **Gunilla** och **Lars** för våra vetenskapliga diskussioner och för ert stora intresse för mina projekt. **Lars** tack för all hjälp med q-PCR och för att du alltid har varit positiv och uppmuntrat mig. Tack **Håkan** för att du har varit en utmärkt examinator. Tack **Zoltan** för språkgranskning.

Tack till alla medförfattare på arbetena, det hade inte gått utan er!

Anders och **Ann-Charlotte** tack för ett bra samarbete. **Börje** och **Sudhirkumar** tack för era diskussioner och ert positiva sätt att se på saker. **Nishtman** tack för all mikroskoperingstiden, och framför allt tack för att du alltid fanns när jag behövde dig. Stort tack till **Kersti** och **Birgit** från *Phase Holographic Imaging* för hjälpen med DH mikroskopet och supporten under alla dessa år.

Jag vill tacka alla doktorander som har funnits under min resas gång. De som har slutat **Anton**, **Cathrine**, **Magnus**, **Yana**, **Peter**, **Mark** och de som är efter **Celina, Dimitri**, **Elena, Olga,** och **Sing** lycka till med er avhandling.

Monzer tack för din hjälp med allt tekniskt, tack för din uppmuntran och din vänlighet. Utan dig hade inget gått! Tack **Vedran** för din hjälp med det tekniska. **Maria** jag är glad att jag fick lära känna dig, tack för all den tid och lycka till med ditt nya jobb.

Ett särskilt tack till mina kära gymnasievänner **Anna**, **Hina, Khoan, Nazira** och **Rachelle**, tack för att ni är så underbara. Tack för att ni alltid påminner mig om andra roliga saker i livet än jobb. Min bästa vän **Falastin,** varje gång vi träffas

rusar tiden iväg och vi hinner aldrig prata färdigt. Tack för allt och lycka till med din avhandling!

Ett stort tack till mina underbara systrar **Amal**, **Safah** och **Wafaa**, tack för att ni alltid finns när jag behöver er ♥ och för att ni alltid bryr er om mig. **Mohammed**, **Ahmed** och **Omar** tack för allt, ni är de bästa bröder man kan önska sig! **Mamma** och **pappa** jag kan nog inte tacka er tillräckligt men tack för att ni får mig alltid att känna att jag klarar allt och att ni är alltid stolta över mig hur det än går. Tack för er hjälp och stöd!

Allra mest vill jag tacka min **Alaeddin,** tack för att du alltid har trott på mig, stöttat mig, uppmuntrat och hjälpt mig. Tack för att du är alltid så snäll och så underbar. **Leith** och **Jasmin** mina älsklingar, ni betyder allt för mig!

REFERENCES

Adamczyk, Barbara, Tharmalingam, Tharmala & Rudd, Pauline M. (2012). Glycans as cancer biomarkers. *Biochimica Et Biophysica Acta (BBA)-General Subjects,* vol. 1820 nr. 9 s. 1347-1353.

Alexander, Cameron, Andersson, Håkan S., Andersson, Lars I., Ansell, Richard J., Kirsch, Nicole, Nicholls, Ian A. et al (2006). Molecular imprinting science and technology: a survey of the literature for the years up to and including 2003. *Journal of Molecular Recognition,* vol. 19 nr. 2 s. 106-180.

Alibek, K., Irving, S., Sautbayeva, Z., Kakpenova, A., Bekmurzayeva, A., Baiken, Y. et al (2014). Disruption of Bcl-2 and Bcl-xL by viral proteins as a possible cause of cancer. *Infectious Agents and Cancer,* vol. 9s. 44-9378-9-44. eCollection 2014.

Alm, Kersti, Cirenajwis, Helena, Gisselsson, Lennart, Gjörloff Wingren, Anette, Janicke, Birgit, Mölder, Anna et al (2011). Digital Holography and Cell Studies. *Holography, Research and Technologies.* (Rosen, Joseph uppl.). Rijeka, Croatia: In Tech. (s. 237-252)

Alm, Kersti, El-Schich, Zahra, Miniotis, Maria F., Wingren, Anette G., Janicke, Birgit & Oredsson, Stina (2013). Cells and Holograms–Holograms and Digital Holographic Microscopy as a Tool to Study the Morphology of Living Cells.

Alonso, Andres, Sasin, Joanna, Bottini, Nunzio, Friedberg, Ilan, Friedberg, Iddo, Osterman, Andrei et al (2004). Protein tyrosine phosphatases in the human genome. *Cell,* vol. 117 nr. 6 s. 699-711.

Amin, HM, Hoshino, K., Yang, H., Lin, Q., Lai, R. & Garcia-Manero, G. (2007). Decreased expression level of SH2 domain-containing protein tyrosine phosphatase-1 (Shp1) is associated with progression of chronic myeloid leukaemia. *The Journal of Pathology,* vol. 212 nr. 4 s. 402-410.

Apollonio, B., Scielzo, C., Bertilaccio, M. T., Ten Hacken, E., Scarfo, L., Ranghetti, P. et al (2013). Targeting B-cell anergy in chronic lymphocytic leukemia. *Blood,* vol. 121 nr. 19 s. 3879-88, S1-8.

Ashkenazi, Avi (2015). Targeting the extrinsic apoptotic pathway in cancer: Lessons learned and future directions. *Journal of Clinical Investigation,* vol. 125 nr. 2 s. 487.

Ashkenazi, Avi & Salvesen, Guy (2014). Regulated cell death: signaling and mechanisms. *Annual Review of Cell and Developmental Biology,* vol. 30s. 337-356.

Baig, S., Seevasant, I., Mohamad, J., Mukheem, A., Huri, HZ & Kamarul, T. (2016). Potential of apoptotic pathway-targeted cancer therapeutic research: Where do we stand&quest. *Cell Death & Disease,* vol. 7 nr. 1 s. e2058.

Baliakas, P., Mattsson, M., Stamatopoulos, K. & Rosenquist, R. (2015). Prognostic indices in chronic lymphocytic leukaemia: where do we stand how do we proceed? *Journal of Internal Medicine,*

Barber, Nicole, Gez, Swetlana, Belov, Larissa, Mulligan, Stephen P., Woolfson, Adrian & Christopherson, Richard I. (2009). Profiling CD antigens on leukaemias with an antibody microarray. *FEBS Letters,* vol. 583 nr. 11 s. 1785-1791.

Belov, Larissa, Mulligan, Stephen P., Barber, Nicole, Woolfson, Adrian, Scott, Mike, Stoner, Kerryn et al (2006). Analysis of human leukaemias and lymphomas using extensive immunophenotypes from an antibody microarray. *British Journal of Haematology,* vol. 135 nr. 2 s. 184-197.

Bergh, A. C., Evaldsson, C., Pedersen, L. B., Geisler, C., Stamatopoulos, K., Rosenquist, R. et al (2014). Silenced B-cell receptor response to autoantigen in a poor-prognostic subset of chronic lymphocytic leukemia. *Haematologica,* vol. 99 nr. 11 s. 1722-1730.

Binet, JL, Auquier, A., Dighiero, G., Chastang, Cl, Piguet, H., Goasguen, J. et al (1981). A new prognostic classification of chronic lymphocytic leukemia derived from a multivariate survival analysis. *Cancer,* vol. 48 nr. 1 s. 198-206.

Blume-Jensen, Peter & Hunter, Tony (2001). Oncogenic kinase signalling. *Nature,* vol. 411 nr. 6835 s. 355-365.

Borrebaeck, Carl A. & Wingren, Christer (2011). Recombinant antibodies for the generation of antibody arrays. *Protein Microarrays*Springer. (s. 247-262)

Brockdorff, Johannes, Williams, Scott, Couture, Clement & Mustelin, Tomas (1999). Dephosphorylation of ZAP-70 and inhibition of T cell activation by activated SHP1. *European Journal of Immunology,* vol. 29 nr. 8 s. 2539-2550.

Buchner, M. & Muschen, M. (2014). Targeting the B-cell receptor signaling pathway in B lymphoid malignancies. *Current Opinion in Hematology,* vol. 21 nr. 4 s. 341-349.

Cambier, John C., Gauld, Stephen B., Merrell, Kevin T. & Vilen, Barbara J. (2007). B-cell anergy: from transgenic models to naturally occurring anergic B cells? *Nature Reviews Immunology,* vol. 7 nr. 8 s. 633-643.

Carl, Daniel, Kemper, Björn, Wernicke, Günther & von Bally, Gert (2004). Parameter-optimized digital holographic microscope for high-resolution living-cell analysis. *Applied Optics,* vol. 43 nr. 36 s. 6536-6544.

Cerutti, Andrea, Puga, Irene & Cols, Montserrat (2011). Innate control of B cell responses. *Trends in Immunology,* vol. 32 nr. 5 s. 202-211.

Chaffer, C. L. & Weinberg, R. A. (2011). A perspective on cancer cell metastasis. *Science (New York, N.Y.),* vol. 331 nr. 6024 s. 1559-1564.

Chakraborty, Arup K. & Weiss, Arthur (2014). Insights into the initiation of TCR signaling. *Nature Immunology,* vol. 15 nr. 9 s. 798-807.

Chalut, Kevin J., Ekpenyong, Andrew E., Clegg, Warren L., Melhuish, Isabel C. & Guck, Jochen (2012). Quantifying cellular differentiation by physical phenotype using digital holographic microscopy. *Integr.Biol.,* vol. 4 nr. 3 s. 280-284.

Chen, L., Widhopf, G., Huynh, L., Rassenti, L., Rai, K. R., Weiss, A. et al (2002). Expression of ZAP-70 is associated with increased B-cell receptor signaling in chronic lymphocytic leukemia. *Blood,* vol. 100 nr. 13 s. 4609-4614.

Chiorazzi, Nicholas, Rai, Kanti R. & Ferrarini, Manlio (2005). Chronic lymphocytic leukemia. *New England Journal of Medicine,* vol. 352 nr. 8 s. 804-815.

Cho, Jaebum, Kushiro, Keiichiro, Teramura, Yuji & Takai, Madoka (2014). Lectin-Tagged Fluorescent Polymeric Nanoparticles for Targeting of Sialic Acid on Living Cells. *Biomacromolecules,* vol. 15 nr. 6 s. 2012-2018.

Coleman, Mathew L., Marshall, Christopher J. & Olson, Michael F. (2004). RAS and RHO GTPases in G1-phase cell-cycle regulation. *Nature Reviews Molecular Cell Biology,* vol. 5 nr. 5 s. 355-366.

Colomb, Tristan, Charrière, Florian, Kühn, Jonas, Marquet, Pierre & Depeursinge, Christian (2008). *Advantages of digital holographic microscopy for real-time full field absolute phase imaging.* Biomedical Optics (BiOS) 2008, International Society for Optics and Photonics s. 686109-686109-10.

Cui, Hongxia, Lin, Yu, Yue, Liling, Zhao, Xuemei & Liu, Jicheng (2011). Differential expression of the α2, 3-sialic acid residues in breast cancer is associated with metastatic potential. *Oncology Reports,* vol. 25 nr. 5 s. 1365-1371.

Cummings, Richard D. (2009). The repertoire of glycan determinants in the human glycome. *Molecular BioSystems,* vol. 5 nr. 10 s. 1087-1104.

Debatin, Klaus-Michael (2004). Apoptosis pathways in cancer and cancer therapy. *Cancer Immunology, Immunotherapy,* vol. 53 nr. 3 s. 153-159.

Delfani, Payam & Wingren, Anette G. (2012). Deep Insight Section. *Http://AtlasGeneticsOncology.Org,* s. 594.

Dennis, J. W., Laferte, S., Yagel, S. & Breitman, M. L. (1989). Asparagine-linked oligosaccharides associated with metastatic cancer. *Cancer Cells (Cold Spring Harbor, N.Y.: 1989),* vol. 1 nr. 3 s. 87-92.

Dexlin-Mellby, Linda, Sandström, Anna, Antberg, Linn, Gunnarsson, Jenny, Hansson, Stefan R., Borrebaeck, Carl A. et al (2011). Design of recombinant antibody microarrays for membrane protein profiling of cell lysates and tissue extracts. *Proteomics,* vol. 11 nr. 8 s. 1550-1554.

Dexlin-Mellby, Linda, Sandström, Anna, Centlow, Magnus, Nygren, Sara, Hansson, Stefan R., Borrebaeck, Carl A. et al (2010). Tissue proteome profiling of preeclamptic placenta using recombinant antibody microarrays. *PROTEOMICS-Clinical Applications,* vol. 4 nr. 10-11 s. 794-807.

Dexlin, Linda, Ingvarsson, Johan, Frendéus, Björn, Borrebaeck, Carl A. & Wingren, Christer (2007). Design of recombinant antibody microarrays for cell surface membrane proteomics. *Journal of Proteome Research,* vol. 7 nr. 01 s. 319-327.

Dighiero, Guillaume & Binet, Jacques-Louis (2000). When and how to treat chronic lymphocytic leukemia. *New England Journal of Medicine,* vol. 343 nr. 24 s. 1799-1801.

Dylke, Janis, Lopes, Jared, Dang-Lawson, May, Machtaler, Steve & Matsuuchi, Linda (2007). Role of the extracellular and transmembrane domain of Ig-α/β in assembly of the B cell antigen receptor (BCR). *Immunology Letters,* vol. 112 nr. 1 s. 47-57.

Eibel, Hermann, Kraus, Helene, Sic, Heiko, Kienzler, Anne-Kathrin & Rizzi, Marta (2014). B cell biology: an overview. *Current Allergy and Asthma Reports,* vol. 14 nr. 5 s. 1-10.

Ellmark, Peter, Högerkorp, Carl-Magnus, Ek, Sara, Belov, L., Berglund, Mattias, Rosenquist, Richard et al (2008). Phenotypic protein profiling of different B cell sub-populations using antibody CD-microarrays. *Cancer Letters,* vol. 265 nr. 1 s. 98-106.

Elmore, S. (2007). Apoptosis: a review of programmed cell death. *Toxicologic Pathology,* vol. 35 nr. 4 s. 495-516.

Else, Monica, Smith, Alastair G., Cocks, Kim, Richards, Sue M., Crofts, Shirley, Wade, Rachel et al (2008). Patients' experience of chronic lymphocytic leukaemia: baseline health-related quality of life results from the LRF CLL4 trial. *British Journal of Haematology,* vol. 143 nr. 5 s. 690-697.

Ferraro, Pietro, Grilli, Simonetta, Alfieri, Domenico, De Nicola, Sergio, Finizio, Andrea, Pierattini, Giovanni et al (2005). Extended focused image in microscopy by digital holography. *Optics Express,* vol. 13 nr. 18 s. 6738-6749.

Ferreira, José A., Videira, Paula A., Lima, Luís, Pereira, Sofia, Silva, Mariana, Carrascal, Mylene et al (2013). Overexpression of tumour-associated carbohydrate antigen sialyl-Tn in advanced bladder tumours. *Molecular Oncology,* vol. 7 nr. 3 s. 719-731.

Fidler, Isaiah J. (2003). The pathogenesis of cancer metastasis: the'seed and soil'hypothesis revisited. *Nature Reviews Cancer,* vol. 3 nr. 6 s. 453-458.

Fischer-Fodor, Eva, Miklasova, Natalia, Berindan-Neagoe, Ioana & Saha, Bhaskar (2015). Iron, inflammation and invasion of cancer cells. *Clujul Medical,* vol. 88 nr. 3 s. 272.

Friedberg, J. W., Sharman, J., Sweetenham, J., Johnston, P. B., Vose, J. M., Lacasce, A. et al (2010). Inhibition of Syk with fostamatinib disodium has significant clinical activity in non-Hodgkin lymphoma and chronic lymphocytic leukemia. *Blood,* vol. 115 nr. 13 s. 2578-2585.

Frigault, M. M., Lacoste, J., Swift, J. L. & Brown, C. M. (2009). Live-cell microscopy - tips and tools. *Journal of Cell Science,* vol. 122 nr. Pt 6 s. 753-767.

Fujita, Takayuki, Satomura, Atsushi, Hidaka, Mutsuko, Ohsawa, Isao, Endo, Morito & Ohi, Hiroyuki (1999). Inhibitory effect of free sialic acid on complement activation and its significance in hypocomplementemic glomerulonephritis. *Journal of Clinical Laboratory Analysis,* vol. 13 nr. 4 s. 173-179.

Fujitani, N., Furukawa, J., Araki, K., Fujioka, T., Takegawa, Y., Piao, J. et al (2013). Total cellular glycomics allows characterizing cells and streamlining the discovery process for cellular biomarkers. *Proceedings of the National Academy of Sciences of the United States of America,* vol. 110 nr. 6 s. 2105-2110.

Fulda, S. & Debatin, KM (2006). Extrinsic versus intrinsic apoptosis pathways in anticancer chemotherapy. *Oncogene,* vol. 25 nr. 34 s. 4798-4811.

Gabor, Dionys (1949). *Microscopy by reconstructed wave-fronts.* Proceedings of the Royal Society of London A: Mathematical, Physical and Engineering Sciences, The Royal Societyvol. 197 nr. 1051 s. 454-487.

Galluzzi, Lorenzo, Vitale, I., Abrams, JM, Alnemri, ES, Baehrecke, EH, Blagosklonny, MV et al (2012a). Molecular definitions of cell death subroutines: recommendations of the Nomenclature Committee on Cell Death 2012. *Cell Death & Differentiation,* vol. 19 nr. 1 s. 107-120.

Galluzzi, L., Kepp, O., Trojel-Hansen, C. & Kroemer, G. (2012b). Mitochondrial control of cellular life, stress, and death. *Circulation Research,* vol. 111 nr. 9 s. 1198-1207.

Gérard, Claude & Goldbeter, Albert (2014). The balance between cell cycle arrest and cell proliferation: control by the extracellular matrix and by contact inhibition. *Interface Focus,* vol. 4 nr. 3 s. 20130075.

Goldar, S., Khaniani, M. S., Derakhshan, S. M. & Baradaran, B. (2015). Molecular mechanisms of apoptosis and roles in cancer development and treatment. *Asian Pacific Journal of Cancer Prevention : APJCP,* vol. 16 nr. 6 s. 2129-2144.

Goldsby, Richard A., Kindt, Thomas J. & Osborne, Barbara A. (2000). Kuby immunology. 4th. *Usa. W,*

Guarini, A., Chiaretti, S., Tavolaro, S., Maggio, R., Peragine, N., Citarella, F. et al (2008). BCR ligation induced by IgM stimulation results in gene expression and functional changes only in IgV H unmutated chronic lymphocytic leukemia (CLL) cells. *Blood,* vol. 112 nr. 3 s. 782-792.

Hallek, M., Cheson, B. D., Catovsky, D., Caligaris-Cappio, F., Dighiero, G., Dohner, H. et al (2008). Guidelines for the diagnosis and treatment of chronic lymphocytic leukemia: a report from the International Workshop on Chronic Lymphocytic Leukemia updating the National Cancer Institute-Working Group 1996 guidelines. *Blood,* vol. 111 nr. 12 s. 5446-5456.

Halverson, Regina, Torres, Raul M. & Pelanda, Roberta (2004). Receptor editing is the main mechanism of B cell tolerance toward membrane antigens. *Nature Immunology,* vol. 5 nr. 6 s. 645-650.

Hamblin, Terry J. (2011). Searching for surrogates for IGHV mutations in chronic lymphocytic leukemia. *Leukemia Research,* vol. 35 nr. 11 s. 1432-1435.

Hanahan, Douglas & Weinberg, Robert A. (2000). The hallmarks of cancer. *Cell,* vol. 100 nr. 1 s. 57-70.

Herishanu, Y., Perez-Galan, P., Liu, D., Biancotto, A., Pittaluga, S., Vire, B. et al (2011). The lymph node microenvironment promotes B-cell receptor signaling, NF-kappaB activation, and tumor proliferation in chronic lymphocytic leukemia. *Blood,* vol. 117 nr. 2 s. 563-574.

Herve, M., Xu, K., Ng, Y. S., Wardemann, H., Albesiano, E., Messmer, B. T. et al (2005). Unmutated and mutated chronic lymphocytic leukemias derive from self-reactive B cell precursors despite expressing different antibody reactivity. *The Journal of Clinical Investigation,* vol. 115 nr. 6 s. 1636-1643.

Hippen, K. L., Schram, B. R., Tze, L. E., Pape, K. A., Jenkins, M. K. & Behrens, T. W. (2005). In vivo assessment of the relative contributions of deletion, anergy, and editing to B cell self-tolerance. *Journal of Immunology (Baltimore, Md.: 1950),* vol. 175 nr. 2 s. 909-916.

Hoebe, RA, Van Oven, CH, Gadella, Th W., Dhonukshe, PB, Van Noorden, CJF & Manders, EMM (2007). Controlled light-exposure microscopy reduces photobleaching and phototoxicity in fluorescence live-cell imaging. *Nature Biotechnology,* vol. 25 nr. 2 s. 249-253.

Hoellenriegel, J., Meadows, S. A., Sivina, M., Wierda, W. G., Kantarjian, H., Keating, M. J. et al (2011). The phosphoinositide 3'-kinase delta inhibitor, CAL-101, inhibits B-cell receptor signaling and chemokine networks in chronic lymphocytic leukemia. *Blood,* vol. 118 nr. 13 s. 3603-3612.

Hoff, S. D., Matsushita, Y., Ota, D. M., Cleary, K. R., Yamori, T., Hakomori, S. et al (1989). Increased expression of sialyl-dimeric LeX antigen in liver metastases of human colorectal carcinoma. *Cancer Research,* vol. 49 nr. 24 Pt 1 s. 6883-6888.

Jaffe, Elaine S. (2001). *Pathology and genetics of tumours of haematopoietic and lymphoid tissues*Iarc.

Jaffe, E. S. (2009). The 2008 WHO classification of lymphomas: implications for clinical practice and translational research. *Hematology / the Education Program of the American Society of Hematology.American Society of Hematology.Education Program,* s. 523-531.

Kaufmann, T., Strasser, A. & Jost, PJ (2012). Fas death receptor signalling: roles of Bid and XIAP. *Cell Death & Differentiation,* vol. 19 nr. 1 s. 42-50.

Kemmler, Manuel, Fratz, Markus, Giel, Dominik, Saum, Norbert, Brandenburg, Albrecht & Hoffmann, Christian (2007). Noninvasive time-dependent cytometry monitoring by digital holography. *Journal of Biomedical Optics,* vol. 12 nr. 6 s. 064002-064002-10.

Kemper, Björn, Bauwens, Andreas, Vollmer, Angelika, Ketelhut, Steffi, Langehanenberg, Patrik, Müthing, Johannes et al (2010). Label-free quantitative cell division monitoring of endothelial cells by digital holographic microscopy. *Journal of Biomedical Optics,* vol. 15 nr. 3 s. 036009-036009-6.

Kemper, Björn, Carl, Daniel, Schnekenburger, Jürgen, Bredebusch, Ilona, Schäfer, Marcus, Domschke, Wolfram et al (2006). Investigation of living pancreas tumor cells by digital holographic microscopy. *Journal of Biomedical Optics,* vol. 11 nr. 3 s. 034005-034005-8.

Khan, Khurum H., Blanco-Codesido, Montserrat & Molife, L. R. (2014). Cancer therapeutics: Targeting the apoptotic pathway. *Critical Reviews in Oncology/Hematology,* vol. 90 nr. 3 s. 200-219.

Khmaladze, Alexander, Matz, Rebecca L., Epstein, Tamir, Jasensky, Joshua, Banaszak Holl, Mark M. & Chen, Zhan (2012). Cell volume changes during apoptosis monitored in real time using digital holographic microscopy. *Journal of Structural Biology,*

Khoury, J. D., Rassidakis, G. Z., Medeiros, L. J., Amin, H. M. & Lai, R. (2004). Methylation of SHP1 gene and loss of SHP1 protein expression are frequent in systemic anaplastic large cell lymphoma. *Blood,* vol. 104 nr. 5 s. 1580-1581.

Klein, Ulf & Dalla-Favera, Riccardo (2008). Germinal centres: role in B-cell physiology and malignancy. *Nature Reviews Immunology,* vol. 8 nr. 1 s. 22-33.

Köhler, Fabian, Hug, Eva, Eschbach, Cathrin, Meixlsperger, Sonja, Hobeika, Elias, Kofer, Juliane et al (2008). Autoreactive B cell receptors mimic autonomous pre-B cell receptor signaling and induce proliferation of early B cells. *Immunity,* vol. 29 nr. 6 s. 912-921.

Kohnke, P. L., Mulligan, S. P. & Christopherson, R. I. (2009). Membrane proteomics for leukemia classification and drug target identification. *Current Opinion in Molecular Therapeutics,* vol. 11 nr. 6 s. 603-610.

Kossev, Plamen M., Raghunath, Puthiyaveettil N., Bagg, Adam, Schuster, Steven, Tomaszewski, John E. & Wasik, Mariusz A. (2001). SHP-1 expression by malignant small B-cell lymphomas reflects the maturation stage of their normal B-cell counterparts. *The American Journal of Surgical Pathology,* vol. 25 nr. 7 s. 949-955.

Koyama, Maho, Oka, Takashi, Ouchida, Mamoru, Nakatani, Yoko, Nishiuchi, Ritsuo, Yoshino, Tadashi et al (2003). Activated proliferation of B-cell lymphomas/leukemias with the SHP1 gene silencing by aberrant CpG methylation. *Laboratory Investigation,* vol. 83 nr. 12 s. 1849-1858.

Kroemer, G., Galluzzi, L., Vandenabeele, Peter, Abrams, J., Alnemri, ES, Baehrecke, EH et al (2009). Classification of cell death: recommendations of the Nomenclature Committee on Cell Death 2009. *Cell Death & Differentiation,* vol. 16 nr. 1 s. 3-11.

Krysko, Dmitri V., Vanden Berghe, Tom, D'Herde, Katharina & Vandenabeele, Peter (2008). Apoptosis and necrosis: detection, discrimination and phagocytosis. *Methods,* vol. 44 nr. 3 s. 205-221.

Kühn, Jonas, Shaffer, Etienne, Mena, Julien, Breton, Billy, Parent, Jérôme, Rappaz, Benjamin et al (2013). Label-free cytotoxicity screening assay by digital holographic microscopy. *Assay and Drug Development Technologies,* vol. 11 nr. 2 s. 101-107.

Kunath, Stephanie, Panagiotopoulou, Maria, Maximilien, Jacqueline, Marchyk, Nataliya, Sänger, Jörg & Haupt, Karsten (2015). Cell and Tissue Imaging with Molecularly Imprinted Polymers as Plastic Antibody Mimics. *Advanced Healthcare Materials,*

Kvansakul, Marc & Hinds, MG (2013). Structural biology of the Bcl-2 family and its mimicry by viral proteins. *Cell Death & Disease,* vol. 4 nr. 11 s. e909.

Lanasa, Mark C. & Weinberg, J. B. (2011). Immunoglobulin class switch recombination in chronic lymphocytic leukemia. *Leukemia & Lymphoma,* vol. 52 nr. 7 s. 1398-1400.

Langlais, C., Hughes, M. A., Cain, K. & MacFarlane, M. (2015). Biochemical Analysis of Initiator Caspase-Activating Complexes: The Apoptosome and the Death-Inducing Signaling Complex. *Cold Spring Harbor Protocols,* vol. 2015 nr. 12 s. pdb.top070326.

LeBien, T. W. & Tedder, T. F. (2008). B lymphocytes: how they develop and function. *Blood,* vol. 112 nr. 5 s. 1570-1580.

Lenart, Thomas, Gustafsson, Mats & Öwall, Viktor (2008). A hardware acceleration platform for digital holographic imaging. *Journal of Signal Processing Systems,* vol. 52 nr. 3 s. 297-311.

Lin, W. W. & Karin, M. (2007). A cytokine-mediated link between innate immunity, inflammation, and cancer. *The Journal of Clinical Investigation,* vol. 117 nr. 5 s. 1175-1183.

Logg, Katarina, Bodvard, Kristofer, Blomberg, Anders & Käll, Mikael (2009). Investigations on light-induced stress in fluorescence microscopy using nuclear localization of the transcription factor Msn2p as a reporter. *FEMS Yeast Research,* vol. 9 nr. 6 s. 875-884.

Logue, S. E. & Martin, S. J. (2008). Caspase activation cascades in apoptosis. *Biochemical Society Transactions,* vol. 36 nr. Pt 1 s. 1-9.

Lu, P., Weaver, V. M. & Werb, Z. (2012). The extracellular matrix: a dynamic niche in cancer progression. *The Journal of Cell Biology,* vol. 196 nr. 4 s. 395-406.

Malumbres, Marcos & Barbacid, Mariano (2001). Milestones in cell division: to cycle or not to cycle: a critical decision in cancer. *Nature Reviews Cancer,* vol. 1 nr. 3 s. 222-231.

Mann, Christopher, Yu, Lingfeng, Lo, Chun-Min & Kim, Myung (2005). High-resolution quantitative phase-contrast microscopy by digital holography. *Optics Express,* vol. 13 nr. 22 s. 8693-8698.

Marquet, Pierre, Rappaz, Benjamin, Magistretti, Pierre J., Cuche, Etienne, Emery, Yves, Colomb, Tristan et al (2005). Digital holographic microscopy: a noninvasive contrast imaging technique allowing quantitative visualization of living cells with subwavelength axial accuracy. *Optics Letters,* vol. 30 nr. 5 s. 468-470.

Mato, Anthony, Jauhar, Shekeab & Schuster, Stephen J. (2015). Management of chronic lymphocytic leukemia (CLL) in the era of B-cell receptor signal transduction inhibitors. *American Journal of Hematology,*

Melchers, F. (2015). Checkpoints that control B cell development. *The Journal of Clinical Investigation,* vol. 125 nr. 6 s. 2203-2210.

Miniotis, Maria F., Mukwaya, Anthonny & Wingren, Anette G. (2014). Digital holographic microscopy for non-invasive monitoring of cell cycle arrest in L929 cells.

Mockridge, C. I., Potter, K. N., Wheatley, I., Neville, L. A., Packham, G. & Stevenson, F. K. (2007). Reversible anergy of sIgM-mediated signaling in the two subsets of CLL defined by VH-gene mutational status. *Blood,* vol. 109 nr. 10 s. 4424-4431.

Mölder, Anna, Sebesta, Mikael, Gustafsson, Mats, Gisselson, L., Wingren, A. G. & Alm, Kersti (2008). Non-invasive, label-free cell counting and quantitative analysis of adherent cells using digital holography. *Journal of Microscopy,* vol. 232 nr. 2 s. 240-247.

Mustelin, Tomas, Vang, Torkel & Bottini, Nunzio (2005). Protein tyrosine phosphatases and the immune response. *Nature Reviews Immunology,* vol. 5 nr. 1 s. 43-57.

Muzio, M., Apollonio, B., Scielzo, C., Frenquelli, M., Vandoni, I., Boussiotis, V. et al (2008). Constitutive activation of distinct BCR-signaling pathways in a subset of CLL patients: a molecular signature of anergy. *Blood,* vol. 112 nr. 1 s. 188-195.

Nair, P., Lu, M., Petersen, S. & Ashkenazi, A. (2014). Apoptosis initiation through the cell-extrinsic pathway. *Methods in Enzymology,* vol. 544s. 99-128.

Neel, Benjamin G., Gu, Haihua & Pao, Lily (2003). The 'Shp'ing news: SH2 domain-containing tyrosine phosphatases in cell signaling. *Trends in Biochemical Sciences,* vol. 28 nr. 6 s. 284-293.

Negro, R., Gobessi, S., Longo, P. G., He, Y., Zhang, Z. Y., Laurenti, L. et al (2012). Overexpression of the autoimmunity-associated phosphatase PTPN22 promotes survival of antigen-stimulated CLL cells by selectively activating AKT. *Blood,* vol. 119 nr. 26 s. 6278-6287.

Nemazee, David (2006). Receptor editing in lymphocyte development and central tolerance. *Nature Reviews Immunology,* vol. 6 nr. 10 s. 728-740.

Ohtsubo, Kazuaki & Marth, Jamey D. (2006). Glycosylation in cellular mechanisms of health and disease. *Cell,* vol. 126 nr. 5 s. 855-867.

Oka, Takashi, Yoshino, Tadashi, Hayashi, Kazuhiko, Ohara, Nobuya, Nakanishi, Tohru, Yamaai, Yuichiro et al (2001). Reduction of hematopoietic cell-specific tyrosine phosphatase SHP-1 gene expression in natural killer cell lymphoma and various types of lymphomas/leukemias: combination analysis with cDNA expression array and tissue microarray. *The American Journal of Pathology,* vol. 159 nr. 4 s. 1495-1505.

Ouyang, L., Shi, Z., Zhao, S., Wang, F-T, Zhou, T-T, Liu, B. et al (2012). Programmed cell death pathways in cancer: a review of apoptosis, autophagy and programmed necrosis. *Cell Proliferation,* vol. 45 nr. 6 s. 487-498.

Packham, G., Krysov, S., Allen, A., Savelyeva, N., Steele, A. J., Forconi, F. et al (2014). The outcome of B-cell receptor signaling in chronic lymphocytic leukemia: proliferation or anergy. *Haematologica,* vol. 99 nr. 7 s. 1138-1148.

Pasparakis, Manolis & Vandenabeele, Peter (2015). Necroptosis and its role in inflammation. *Nature,* vol. 517 nr. 7534 s. 311-320.

Pavillon, Nicolas, Kühn, Jonas, Moratal, Corinne, Jourdain, Pascal, Depeursinge, Christian, Magistretti, Pierre J. et al (2012). Early cell death detection with digital holographic microscopy. *PloS One,* vol. 7 nr. 1 s. e30912.

Phan, T. G., Amesbury, M., Gardam, S., Crosbie, J., Hasbold, J., Hodgkin, P. D. et al (2003). B cell receptor-independent stimuli trigger immunoglobulin (Ig) class switch recombination and production of IgG autoantibodies by anergic self-reactive B cells. *The Journal of Experimental Medicine,* vol. 197 nr. 7 s. 845-860.

Pieper, Kathrin, Grimbacher, Bodo & Eibel, Hermann (2013). B-cell biology and development. *Journal of Allergy and Clinical Immunology,* vol. 131 nr. 4 s. 959-971.

Ponader, S., Chen, S. S., Buggy, J. J., Balakrishnan, K., Gandhi, V., Wierda, W. G. et al (2012). The Bruton tyrosine kinase inhibitor PCI-32765 thwarts chronic lymphocytic leukemia cell survival and tissue homing in vitro and in vivo. *Blood,* vol. 119 nr. 5 s. 1182-1189.

Poole, Alastair W. & Jones, Matthew L. (2005). A SHPing tale: perspectives on the regulation of SHP-1 and SHP-2 tyrosine phosphatases by the C-terminal tail. *Cellular Signalling,* vol. 17 nr. 11 s. 1323-1332.

Quach, T. D., Manjarrez-Orduno, N., Adlowitz, D. G., Silver, L., Yang, H., Wei, C. et al (2011). Anergic responses characterize a large fraction of human autoreactive naive B cells expressing low levels of surface IgM. *Journal of Immunology (Baltimore, Md.: 1950),* vol. 186 nr. 8 s. 4640-4648.

Rai, K. R., Sawitsky, A., Cronkite, E. P., Chanana, A. D., Levy, R. N. & Pasternack, B. S. (1975). Clinical staging of chronic lymphocytic leukemia. *Blood,* vol. 46 nr. 2 s. 219-234.

Rappaz, Benjamin, Marquet, Pierre, Cuche, Etienne, Emery, Yves, Depeursinge, Christian & Magistretti, Pierre (2005). Measurement of the integral refractive index and dynamic cell morphometry of living cells with digital holographic microscopy. *Optics Express,* vol. 13 nr. 23 s. 9361-9373.

Reth, M. & Nielsen, P. (2014). Signaling circuits in early B-cell development. *Advances in Immunology,* vol. 122s. 129-175.

Reubold, Thomas F. & Eschenburg, Susanne (2012). A molecular view on signal transduction by the apoptosome. *Cellular Signalling,* vol. 24 nr. 7 s. 1420-1425.

Rosén, Anders, Bergh, Ann-Charlotte, Gogok, Peter, Evaldsson, Chamilly, Myhrinder, Anna L., Hellqvist, Eva et al (2012). Lymphoblastoid cell line with B1 cell characteristics established from a chronic lymphocytic leukemia clone by in vitro EBV infection. *Oncoimmunology,* vol. 1 nr. 1 s. 18-27.

Rosenspire, Allen J. & Chen, Kang (2015). Anergic B Cells: Precarious On-Call Warriors at the Nexus of Autoimmunity and False-Flagged Pathogens. *Frontiers in Immunology,* vol. 6

Rosenwald, A., Alizadeh, A. A., Widhopf, G., Simon, R., Davis, R. E., Yu, X. et al (2001). Relation of gene expression phenotype to immunoglobulin mutation genotype in B cell chronic lymphocytic leukemia. *The Journal of Experimental Medicine,* vol. 194 nr. 11 s. 1639-1647.

Rozman, Ciril & Montserrat, Emilio (1995). Chronic lymphocytic leukemia. *New England Journal of Medicine,* vol. 333 nr. 16 s. 1052-1057.

Samraj, Annie N., Läubli, Heinz, Varki, Nissi & Varki, Ajit (2014). Involvement of a non-human sialic acid in human cancer. *Frontiers in Oncology,* vol. 4

Sebesta, Mikael & Gustafsson, Mats (2005). Object characterization with refractometric digital Fourier holography. *Optics Letters,* vol. 30 nr. 5 s. 471-473.

Seidenfaden, R., Krauter, A., Schertzinger, F., Gerardy-Schahn, R. & Hildebrandt, H. (2003). Polysialic acid directs tumor cell growth by controlling heterophilic neural cell adhesion molecule interactions. *Molecular and Cellular Biology,* vol. 23 nr. 16 s. 5908-5918.

Sen, Goutam, Bikah, Gabriel, Venkataraman, Chandrasekar & Bondada, Subbarao (1999). Negative regulation of antigen receptor-mediated signaling by constitutive association of CD5 with the SHP-1 protein tyrosine phosphatase in B-1 B cells. *European Journal of Immunology,* vol. 29s. 3319-3328.

Sessler, Tamas, Healy, Sandra, Samali, Afshin & Szegezdi, Eva (2013). Structural determinants of DISC function: new insights into death receptor-mediated apoptosis signalling. *Pharmacology & Therapeutics,* vol. 140 nr. 2 s. 186-199.

Shinde, Sudhirkumar, El-Schich, Zahra, Malakpour, Atena, Wan, Wei, Dizeyi, Nishtman, Mohammadi, Reza et al (2015). Sialic Acid-Imprinted Fluorescent Core–Shell Particles for Selective Labeling of Cell Surface Glycans. *Journal of the American Chemical Society,* vol. 137 nr. 43 s. 13908-13912.

Siddon, A. J., Rinder, H. M. & Education Committee of the Academy of Clinical Laboratory Physicians and Scientists (2013). Pathology consultation on evaluating prognosis in incidental monoclonal lymphocytosis and chronic lymphocytic leukemia. *American Journal of Clinical Pathology,* vol. 139 nr. 6 s. 708-712.

Sivina, M., Hartmann, E., Kipps, T. J., Rassenti, L., Krupnik, D., Lerner, S. et al (2011). CCL3 (MIP-1alpha) plasma levels and the risk for disease progression in chronic lymphocytic leukemia. *Blood,* vol. 117 nr. 5 s. 1662-1669.

Slupsky, J. R. (2014). Does B cell receptor signaling in chronic lymphocytic leukaemia cells differ from that in other B cell types? *Scientifica,* vol. 2014s. 208928.

Stybayeva, Gulnaz, Mudanyali, Onur, Seo, Sungkyu, Silangcruz, Jaime, Macal, Monica, Ramanculov, Erlan et al (2010). Lensfree holographic imaging of antibody microarrays for high-throughput detection of leukocyte numbers and function. *Analytical Chemistry,* vol. 82 nr. 9 s. 3736-3744.

Tangvoranuntakul, P., Gagneux, P., Diaz, S., Bardor, M., Varki, N., Varki, A. et al (2003). Human uptake and incorporation of an immunogenic nonhuman dietary sialic acid. *Proceedings of the National Academy of Sciences of the United States of America,* vol. 100 nr. 21 s. 12045-12050.

Taylor, Rebecca C., Cullen, Sean P. & Martin, Seamus J. (2008). Apoptosis: controlled demolition at the cellular level. *Nature Reviews Molecular Cell Biology,* vol. 9 nr. 3 s. 231-241.

Tchikov, Vladimir, Bertsch, Uwe, Fritsch, Jürgen, Edelmann, Bärbel & Schütze, Stefan (2011). Subcellular compartmentalization of TNF receptor-1 and CD95 signaling pathways. *European Journal of Cell Biology,* vol. 90 nr. 6 s. 467-475.

Tibaldi, E., Brunati, AM, Zonta, F., Frezzato, F., Gattazzo, C., Zambello, R. et al (2011). Lyn-mediated SHP-1 recruitment to CD5 contributes to resistance to apoptosis of B-cell chronic lymphocytic leukemia cells. *Leukemia,* vol. 25 nr. 11 s. 1768-1781.

Tokoyoda, Koji, Hauser, Anja E., Nakayama, Toshinori & Radbruch, Andreas (2010). Organization of immunological memory by bone marrow stroma. *Nature Reviews Immunology,* vol. 10 nr. 3 s. 193-200.

Tokoyoda, Koji, Zehentmeier, Sandra, Chang, Hyun-Dong & Radbruch, Andreas (2009). Organization and maintenance of immunological memory by stroma niches. *European Journal of Immunology,* vol. 39 nr. 8 s. 2095-2099.

Tonks, Nicholas K. (2013). Protein tyrosine phosphatases–from housekeeping enzymes to master regulators of signal transduction. *Febs Journal,* vol. 280 nr. 2 s. 346-378.

Torre, Lindsey A., Bray, Freddie, Siegel, Rebecca L., Ferlay, Jacques, Lortet-Tieulent, Joannie & Jemal, Ahmedin (2015). Global cancer statistics, 2012. *CA: A Cancer Journal for Clinicians,* vol. 65 nr. 2 s. 87-108.

Trulsson, Maria, Yu, Hao, Gisselsson, Lennart, Chao, Yinxia, Urbano, Alexander, Aits, Sonja et al (2011). HAMLET binding to α-actinin facilitates tumor cell detachment.

van Horssen, Remco, Buccione, Roberto, Willemse, Marieke, Cingir, Sahika, Wieringa, Bé & Attanasio, Francesca (2013). Cancer cell metabolism regulates extracellular matrix degradation by invadopodia. *European Journal of Cell Biology,* vol. 92 nr. 3 s. 113-121.

Vaque, J. P., Martinez, N., Batlle-Lopez, A., Perez, C., Montes-Moreno, S., Sanchez-Beato, M. et al (2014). B-cell lymphoma mutations: improving diagnostics and enabling targeted therapies. *Haematologica,* vol. 99 nr. 2 s. 222-231.

Varki, A. & Lowe, J. B. (2009). Biological Roles of Glycans. Ingår i A. Varki et al. (red.), *Essentials of Glycobiology* (2nd uppl.). Cold Spring Harbor (NY): The Consortium of Glycobiology Editors, La Jolla, California.

Varki, N. M. & Varki, A. (2002). Heparin inhibition of selectin-mediated interactions during the hematogenous phase of carcinoma metastasis: rationale for clinical studies in humans. *Seminars in Thrombosis and Hemostasis,* vol. 28 nr. 1 s. 53-66.

Vasapollo, Giuseppe, Sole, Roberta D., Mergola, Lucia, Lazzoi, Maria R., Scardino, Anna, Scorrano, Sonia et al (2011). Molecularly imprinted polymers: present and future prospective. *International Journal of Molecular Sciences,* vol. 12 nr. 9 s. 5908-5945.

Victora, Gabriel D. & Nussenzweig, Michel C. (2012). Germinal centers. *Annual Review of Immunology,* vol. 30s. 429-457.

Vollbrecht, Claudia, Mairinger, Fabian D., Koitzsch, Ulrike, Peifer, Martin, Koenig, Katharina, Heukamp, Lukas C. et al (2015). Comprehensive Analysis of Disease-Related Genes in Chronic Lymphocytic Leukemia by Multiplex PCR-Based Next Generation Sequencing. *PloS One,* vol. 10 nr. 6 s. e0129544.

Wang, Feng-Ling, Cui, Shu-Xiang, Sun, Lan-Ping, Qu, Xian-Jun, Xie, Yan-Ying, Zhou, Ling et al (2009). High expression of α 2, 3-linked sialic acid residues is associated with the metastatic potential of human gastric cancer. *Cancer Detection and Prevention,* vol. 32 nr. 5 s. 437-443.

Wang, Yunxin, Yang, Yishu, Wang, Dayong, Ouyang, Liting, Zhang, Yizhuo, Zhao, Jie et al (2013). Morphological measurement of living cells in methanol with digital holographic microscopy. *Computational and Mathematical Methods in Medicine,* vol. 2013

Weibrecht, Irene, Böhmer, Sylvia-Annette, Dagnell, Markus, Kappert, Kai, Östman, Arne & Böhmer, Frank-D (2007). Oxidation sensitivity of the catalytic cysteine of the protein-tyrosine phosphatases SHP-1 and SHP-2. *Free Radical Biology and Medicine,* vol. 43 nr. 1 s. 100-110.

Westphal, Dana, Dewson, Grant, Czabotar, Peter E. & Kluck, Ruth M. (2011). Molecular biology of Bax and Bak activation and action. *Biochimica Et Biophysica Acta (BBA)-Molecular Cell Research,* vol. 1813 nr. 4 s. 521-531.

Whitcombe, Michael J., Chianella, Iva, Larcombe, Lee, Piletsky, Sergey A., Noble, James, Porter, Robert et al (2011). The rational development of molecularly imprinted polymer-based sensors for protein detection. *Chemical Society Reviews,* vol. 40 nr. 3 s. 1547-1571.

Wiestner, A., Rosenwald, A., Barry, T. S., Wright, G., Davis, R. E., Henrickson, S. E. et al (2003). ZAP-70 expression identifies a chronic lymphocytic leukemia subtype with unmutated immunoglobulin genes, inferior clinical outcome, and distinct gene expression profile. *Blood,* vol. 101 nr. 12 s. 4944-4951.

Wilkinson, Adam C. & Göttgens, Berthold (2013). Transcriptional regulation of haematopoietic stem cells. *Transcriptional and Translational Regulation of Stem Cells*Springer. (s. 187-212)

Wingren, Christer, James, Peter & Borrebaeck, Carl A. (2009). Strategy for surveying the proteome using affinity proteomics and mass spectrometry. *Proteomics,* vol. 9 nr. 6 s. 1511-1517.

Wong, RS (2011). Apoptosis in cancer: from pathogenesis to treatment. *J Exp Clin Cancer Res,* vol. 30 nr. 1 s. 87.

Wu, Chengyu, Sun, Mingzhong, Liu, Lijun & Zhou, G. W. (2003). The function of the protein tyrosine phosphatase SHP-1 in cancer. *Gene,* vol. 306s. 1-12.

Xiao, Xudong & Puri, Ishwar K. (2002). Digital recording and numerical reconstruction of holograms: an optical diagnostic for combustion. *Applied Optics,* vol. 41 nr. 19 s. 3890-3899.

Yarkoni, Yuval, Getahun, Andrew & Cambier, John C. (2010). Molecular underpinning of B-cell anergy. *Immunological Reviews,* vol. 237 nr. 1 s. 249-263.

Yu, Lingfeng, Mohanty, Samarendra, Zhang, Jun, Genc, Suzanne, Kim, Myung K., Berns, Michael W. et al (2009). Digital holographic microscopy for quantitative cell dynamic evaluation during laser microsurgery. *Optics Express,* vol. 17 nr. 14 s. 12031-12038.

Yu, P., Mustata, M., Turek, JJ, French, PMW, Melloch, MR & Nolte, DD (2003). Holographic optical coherence imaging of tumor spheroids. *Applied Physics Letters,* vol. 83 nr. 3 s. 575-577.

Zimmer, Alexandra S. & Steeg, Patricia S. (2015). Meaningful prevention of breast cancer metastasis: candidate therapeutics, preclinical validation, and clinical trial concerns. *Journal of Molecular Medicine,* vol. 93 nr. 1 s. 13-29.

PAPER I-IV

III

Journal of Structural Biology 189 (2015) 207–212

Contents lists available at ScienceDirect

Journal of Structural Biology

journal homepage: www.elsevier.com/locate/yjsbi

Induction of morphological changes in death-induced cancer cells monitored by holographic microscopy

Zahra El-Schich [a], Anna Mölder [b], Helena Tassidis [c], Pirkko Härkönen [d], Maria Falck Miniotis [a], Anette Gjörloff Wingren [a,*]

[a] Department of Biomedical Science, Health and Society, Malmö University, Malmö, Sweden
[b] Phase Holographic Imaging AB, Lund, Sweden
[c] Department of Natural Science, Kristianstad University, Kristianstad, Sweden
[d] Department of Cell Biology and Anatomy, Institute of Biomedicine, University of Turku, Turku, Finland

ARTICLE INFO

Article history:
Received 7 October 2014
Received in revised form 16 January 2015
Accepted 17 January 2015
Available online 28 January 2015

Keywords:
Digital holographic microscopy
Volume
Cell death
Viability
Cell morphology
Imaging

ABSTRACT

We are using the label-free technique of holographic microscopy to analyze cellular parameters including cell number, confluence, cellular volume and area directly in the cell culture environment. We show that death-induced cells can be distinguished from untreated counterparts by the use of holographic microscopy, and we demonstrate its capability for cell death assessment. Morphological analysis of two representative cell lines (L929 and DU145) was performed in the culture flasks without any prior cell detachment. The two cell lines were treated with the anti-tumour agent etoposide for 1–3 days. Measurements by holographic microscopy showed significant differences in average cell number, confluence, volume and area when comparing etoposide-treated with untreated cells. The cell volume of the treated cell lines was initially increased at early time-points. By time, cells decreased in volume, especially when treated with high doses of etoposide. In conclusion, we have shown that holographic microscopy allows label-free and completely non-invasive morphological measurements of cell growth, viability and death. Future applications could include real-time monitoring of these holographic microscopy parameters in cells in response to clinically relevant compounds.

1. Introduction

Cancer is the second leading cause of death both within the EU as well as in America and it is a remarkably heterogeneous disease that is characterized by unrestrained cell growth and division (Jemal et al., 2011). A key challenge for researchers is to unravel the full spectra of intricate mechanisms that drive cancer growth, in order to aid the development of highly efficacious cancer treatments that will improve prognosis and overall survival of the patient. The loss of balance between cell viability and cell death in cancer is a widely studied subject among cell biologists. There are two types of cell death, apoptosis and necrosis. Apoptosis is an orchestrated process of programmed cell death in vertebrates that plays a central role in development and homeostasis, whereas necrosis is the form of cell injury that results in the premature death of cells in living tissue. The mechanism of apoptosis is complex and involves many pathways (Wong, 2011). Morphologically, dying cells differ vastly from viable cells in several aspects (Kroemer et al., 2005). Specific morphological features, in particular volume changes accompany cell death processes and are often used to define the different cell death pathways (Krysko et al., 2008).

Holographic microscopy is an approach for label-free non-invasive imaging of cultured cells, in order to monitor growth, viability and death. The technique is non-destructive and a non-phototoxic method, allowing the user to perform both qualitative and quantitative measurements of living cells over time. In comparison to techniques that measure extracellular release of markers, such as cell staining methods, and the western blot technique, holographic microscopy enable the users to non-invasively collect information on cellular area, confluence, shape, optical thickness and cell volume which can give an indirect measurement of cell volume (Ferraro et al., 2005; Charrière et al., 2006; Carl et al., 2004; Kemper et al., 2006; Rappaz et al., 2005; Mann et al., 2005; Chalut et al., 2012). Since the first studies on living cells, holographic microscopy has been used to study a wide range of different cell types, e.g. protozoa, bacteria and plant cells, mammalian cells such as nerve cells, stem cells, various tumor cells, bacterial–cell interactions, red blood cells and sperm cells (reviewed in Alm et al., 2013).

* Corresponding author.
E-mail address: anette.gjorloff-wingren@mah.se (A. Gjörloff Wingren).

http://dx.doi.org/10.1016/j.jsb.2015.01.010
1047-8477/

It is also possible to use holographic microscopy for counting of adherent cells (Mölder et al., 2008). Four different adherent human cell lines were investigated by analyzing cells daily for up to 4 days. By performing measurements over time with holographic microscopy, changes in proliferation pattern were recorded showing high correlation with manual cell counting.

Recent holographic microscopy studies have shown that the technique can be used to monitor cell changes in PanC-1 pancreatic cancer cells, cell death in single DU145 prostate cancer cells (Alm et al., 2013) as well as in microgravity-induced cell cycle alterations in MLO-Y4 osteocytes (Pan et al., 2012). Moreover, holographic microscopy has been utilized for analysis of staurosporine-induced cell death in human epithelial KB cells (Khmaladze et al., 2012) and in studies of cell death triggered by excessive stimulation of neurotransmitters in primary cultures of mouse cortical neurons (Pavillon et al., 2012). Using cervical cancer cell line, HeLa and Chinese hamster ovary cell line, CHO-K1, Kuhn and co-workers described how the technique can be used for cytotoxic screening for high-throughput purposes (Kühn et al., 2013). Indeed, the use of holographic microscopy as a fast, automatic, and cost efficient evaluation tool for different cancer treatments is promising (Rappaz et al., 2014).

Here we show that morphological cellular changes, such as volume and area, induced by the chemotherapeutic anti-cancer drug etoposide can be identified by monitoring with holographic microscopy. We present data on measurements of growing cells, proliferation, and dying cells, cell death induction, of L929 mouse fibroblast cells and DU145 human prostate cancer cells.

2. Materials and methods

2.1. Cell lines and culture

L929 mouse fibroblast and DU145 human prostate cancer cells were obtained from The American Type Culture Collection (ATCC/LGC Standards, Teddington, UK). L929 cells were cultured in Minimal Essential Medium (MEM) with 1% Non-Essential amino acids, HEPES Buffer Solution 1 M, L-glutamine 200 mM, 10% fetal calf serum (FCS) and 1% penicillin/streptomycin. DU145 cells were cultured in Dulbecco's Modified Eagle Medium (DMEM) with 1 g/l glucose, 1% sodium pyruvate, 1% glutamine supplemented and 10% FCS and incubated at 37 °C in a humidified atmosphere containing 5% CO_2 (medium and supplements were obtained from Invitrogen, Carlsbad, CA, USA).

2.2. Reagents

Etoposide was dissolved in dimethyl sulfoxide (DMSO, Sigma–Aldrich Co., St. Louis, USA) and used at a final concentration of 1, 5 and 10 μM. 2×10^5 L929 cells and 2×10^3 cells were seeded into 25 cm^2 flasks or 96-well plates, respectively. After 24 h, cells were treated with etoposide and incubated for another 24, 48 and 72 h.

2.3. Cell viability measurements

Different concentrations of cells were seeded. L929 cells were seeded at 50,000; 100,000; 150,000 or 200,000 and DU145 were seeded at 150,000; 200,000; 250,000 or 300,000 into 25 cm^2 flasks and allowed to adhere for 24 h. Following adherence, cell growth was monitored with holographic microscopy over time, for 24, 48, 72 and 96 h. For cell death studies of L929 and DU145, 2,000 cells were seeded in 96-well plates with 100 μl of DMEM or MEM medium respectively, and incubated for 24 h. Cells were then treated with etoposide as described previously under Section 2.2. Post-treatment, MTS-assay was performed by adding 20 μl of MTS/PMS solution CellTiter 96® AQueous Non-Radioactive Cell Proliferation Assay, Promega Corporation, Madison, USA) to the desired wells and plates were then incubated for 2 h. The absorbance was measured at 490 nm by using BIO-TEK® micro plate reader.

2.4. Digital holographic microscopy measurements

Following treatment with etoposide, holographic microscopy images were acquired using Holomonitor™ M3 (Phase Holographic Imaging AB, PHIAB, Lund, Sweden) equipped with a 0.8 mW HeNe laser (633 nm). The laser intensity for this system is approximately 10 W/m^2 during imaging and the exposure time is less than 5 ms (Gustafsson et al., 2004; Gustafsson and Sebesta, 2004). In the M3 Holomonitor system, the laser ray is divided into two beams, an object beam passing through the sample and a reference beam. By combining both object- and reference beams together on a CCD camera digital sensor, an interference pattern is created.

2.5. Computer software

The fully automated computer algorithm *Hstudio* (PHIAB) is established by a standard Fresnel approximation and reconstructs the interference shape (created of the reflected light of the object) into a holographic image (Cuche et al., 1999), with unwrapped focal plane which construct a planar background (Sebesta and Gustafsson, 2005).

The focal plane is automatically estimated by quadratic minimization of the variance of the amplitude image (Dubois et al., 2006). The phase image at the focal plane is unwrapped using Flyn's unwrapping algorithm (Ghiglia and Pritt, 1998) and fitted to a second-order polynomial to construct an approximately planar background (Sebesta and Gustafsson, 2005; Miccio et al., 2007).

Several were captured from each individual sample. Image areas covered with cells were then segmented using a watershed-based algorithm, yielding data on cell number, confluence, cell volume and cell area could be obtained (Mölder et al., 2008). For absolute values of refraction indexes for cells and culture medium, assumptions were included in the automated computer algorithm *Hstudio*. As the laser intensity is only approximately 10 W/m^2 during imaging, and the exposure time is less than 0.5 s, it is assumed that the laser irradiation has only minimal effects on the physiological functions of the cells (Mölder et al., 2008; Hawkins and Abrahamse, 2006; Logg et al., 2009; Tinevez et al., 2012).

2.6. Statistical methods

Mean and standard deviation were used for statistical analysis of all calculations. For the cell proliferation and apoptosis studies, at least 20 images per sample were captured from at least two individual experiments. The error bars shown in the images were calculated as the standard deviation between individual images.

3. Results

3.1. Measurements of cell growth curves using holographic microscopy

Different concentrations of L929 cells (50,000–200,000) and DU145 cells (150,000–300,000) were seeded and measured after 24–96 h. The number of cells per area unit (Fig. 1A and B) and the confluence in % per area unit (Fig. 1C and D) were calculated by digital holography. The number of cells and the confluence increased over time for L929 and DU145 cells.

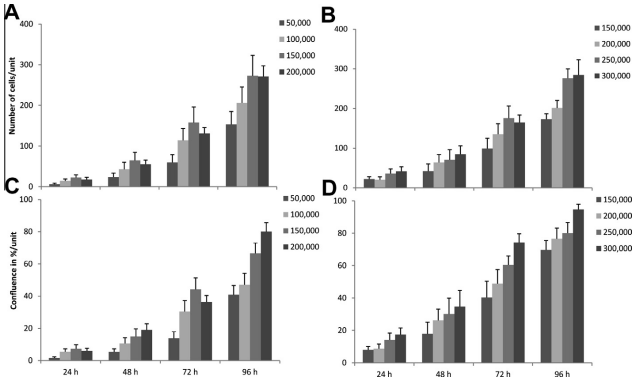

Fig.1. L929 and DU145 cells were seeded at different cell concentrations and measured over time, 24, 48, 72, and 96 h. The number of cells (A and B) and the confluence in % (C and D) were calculated for L929 cells (A and C) and DU145 cells (B and D), respectively, using holographic microscopy. Error bars are based of the total number of images.

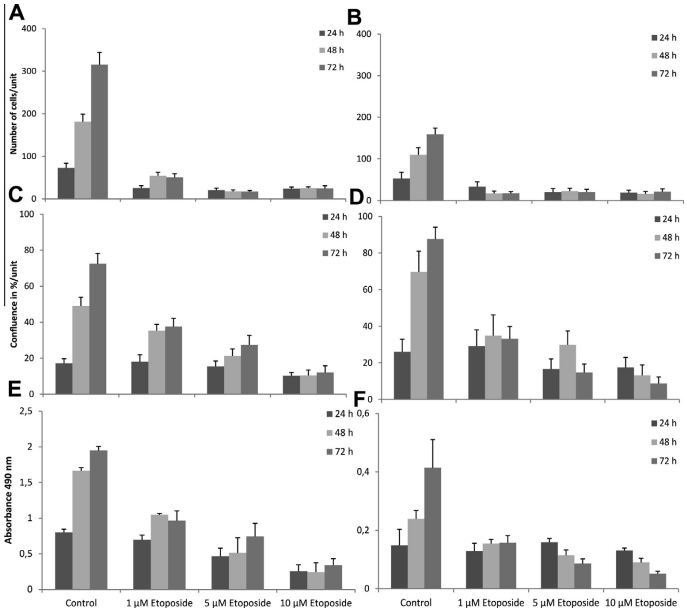

Fig.2. L929 and DU145 cells were treated with etoposide (1, 5, and 10 µM) or left untreated (control) and measured after 24, 48, and 72 h. After computer reconstruction, the images were segmented in order to perform a cell count, and the number of L929 and DU145 cells were estimated per area unit (A and B) and the confluence in % (C and D). L929 cells are shown in A and C, and DU145 cells are shown in B and D. Cell viability was also measured with an MTS assay on treated and untreated L929 (E) and DU145 (F) after 24, 48, and 72 h. Error bars are based on the total number of images.

3.2. Measurements of viability, cell number and confluence

Induction of cell death was analyzed after 24, 48 and 72 h treatments with 1, 5 and 10 µM etoposide in L929 and DU145 cells. Concentrations of etoposide higher than 10 µM killed both cell lines already after 24 h incubation. The number of control cells per area units increased over time, while for treated cells, the numbers of cells was unchanged over time (Fig. 2A and B). The confluence in percent per area units increased for L929 control cells over time, while a minor increase of the confluence was obtained over

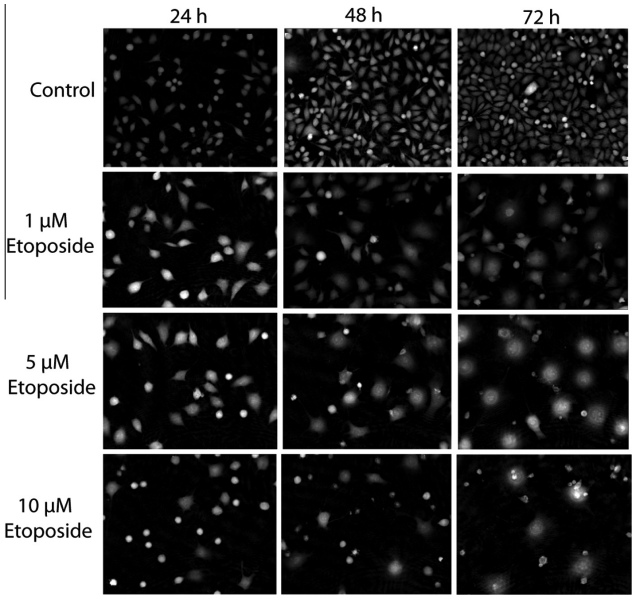

Fig.3. L929 mouse fibroblast cells were treated with etoposide (1, 5 and 10 µM) or left untreated, control. Images of the cells were captured using holographic microscopy after 24, 48 and 72 h, respectively. Hologram pictures show the morphology changes over time with the different concentrations of etoposide.

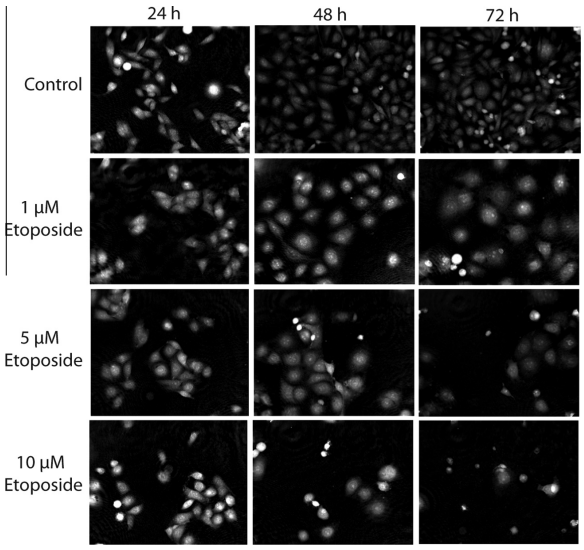

Fig.4. DU145 prostate cancer cells were treated with etoposide (1, 5 and 10 µM) or left untreated. Images of the cells were captured by holographic microscopy after 24, 48 and 72 h, respectively. Hologram pictures show the morphology changes over time with the different concentrations of etoposide.

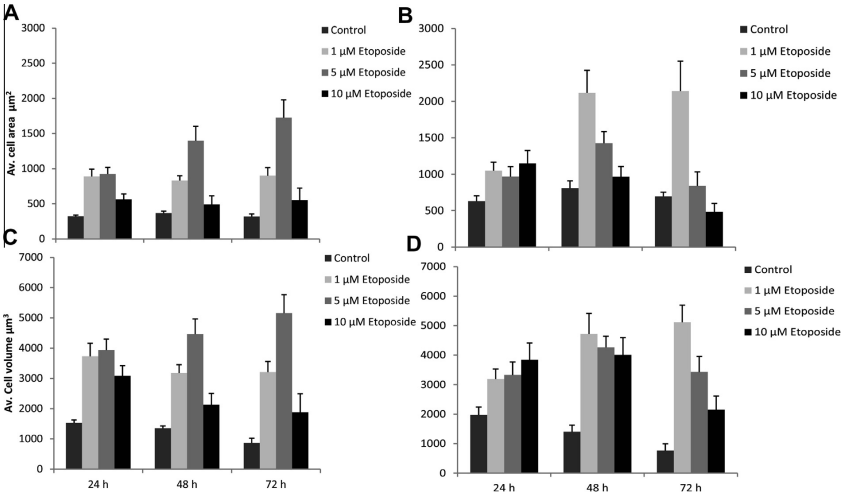

Fig.5. Images of L929 and DU145 cells were captured by Holomonitor™ M3. The cells were treated with etoposide (1, 5 and 10 µM), or left untreated, for 3 days and a hologram was captured after 24, 48 and 72 h. The mean cell area (A and B) and the mean cell volume (C and D) were calculated using holographic microscopy images. L929 cells are shown in A and C, and DU145 cells are shown in B and D. Error bars are based of the total number of images.

time in the treated cells (1 and 5 µM etoposide). For 10 µM etoposide treated cells, the confluence was unchanged over time (Fig. 2C). For DU145 control cells, the confluence increased over time, while for cells treated with 1 µM etoposide, the confluence remained unchanged over time. For cells treated with 5 µM etoposide, the confluence increased after 48 h and decreased after 72 h. For 10 µM etoposide treated cells, the confluence decreased at all time-points (Fig. 2D).

To confirm the ability to use holographic microscopy for cell viability, an MTS-assay was performed. L929 and DU145 cells were treated and analyzed after 24, 48 and 72 h. The L929 and DU145 cell viability increased over time for control cells and decreased for treated cells. For etoposide concentrations less than 1 µM, the viability for DU145 decreased, whereas for L929 the viability increased but at a much lower rate, compared to the control (Fig. 2E and F). The addition of the drug vehicle DMSO had no effect on the parameters investigated in this study (data not shown).

3.3. Morphological changes in hologram images

The morphology of etoposide treated L929 and DU145 cells changed after 24–72 h compared to untreated cells. The cell area increased and the number of cells decreased compared to the untreated cells (Figs. 3 and 4). As seen in the hologram images, the morphological changes were both time dependent and etoposide concentration dependent.

3.4. Measurements of the mean cell area and the mean cell volume with digital holography

The mean cell area and the mean cell volume were also measured with digital holography. While the cell volume decreased, there were no major changes of the L929 and DU145 cell area for untreated cells over time. However, L929 and DU145 cells treated with 1 and 5 µM etoposide showed an increased cell area (Fig. 5A and B) and cell volume (Fig. 5C and D) compared to untreated cells, while the cells treated with 10 µM etoposide showed decreased cell area and volume.

4. Discussion

In the current study investigating morphological changes in two cell lines using holographic microscopy, we undertook the same strategy as in a previous study when counting cells using the same method (Mölder et al., 2008). By first optimizing the cell growth curves for viable cells with holographic microscopy, we could determine the morphological changes after etoposide-treatment over time.

Here we show the results of careful measurements on cell populations, analyzed with holographic microscopy and the commonly used MTS viability assay. The growth curves obtained with holographic microscopy and MTS assay were very similar. With holographic microscopy, we are able to show that untreated control cells could be distinguished from etoposide-treated death-induced cells by determining cell number, confluence and morphological alterations such as cell area and volume. When treating the cells with the lowest dose of etoposide, 1 µM, the number of both L929 and DU145 cells decreased already at 24 h, which was the first time point analyzed. The overall decrease in cell number was both time dependent and concentration dependent, and was more prominent when analyzing cell confluence, especially at the lower doses of etoposide. Indeed, this is due to the initial swelling of the dying cells, resulting in an increase of both the cell area and volume of the L929 and DU145 cells at etoposide concentrations of 1 and 5 µM, respectively. Only the high dose of etoposide (10 µM) induced an initial decrease in the cell area and volume.

The results shown in this study are on cell populations, but single cells can also be analyzed. We have previously analyzed and monitored individual cells treated with etoposide at early time-points by holographic microscopy. DU145 cells that contracted

became dense and rounded up after approximately 4 h of treatment (Alm et al., 2013). Thereafter, the cells became uneven and 5.5 h after the beginning of etoposide treatment, the cells fragmented. Interestingly, the remnants of the cell body contracted into a smaller cell-like structure that resembled an apoptotic body. The fragmentation of the cell is a classic hallmark of apoptosis.

Cell volume regulation of neuronal cells has been monitored by holographic microscopy phase response, which allowed estimations in a very short time-frame (Pavillon et al., 2012; Rappaz et al., 2014). By varying the concentration and exposure time of L-glutamate to primary cultures of mouse cortical neurons, Pavillon et al. could identify reversible phase responses corresponding to phase recovery though an efficient ionic homeostasis. By monitoring the phase shift, nuclear condensation and "blebbing" induced by treatment was distinguished, which could indicate that cells were apoptotic rather than necrotic. Importantly, cells recognized within minutes by their holographic microscopy phase signal as unable to regulate their ionic homeostasis, were only several hours later identified as dead by trypan blue staining. Interestingly, Rappaz et al., compared holographic microscopy with both differential interference contrast (DIC) and transport of intensity equation (TIE) and showed the advantages with holographic microscopy for automated phenotypic drug screening (Rappaz et al., 2014). Moreover, Khmaladze and colleagues used holographic microscopy to measure early stage morphological features of apoptosis in cells, which were associated with a marked decrease in cell volume (Khmaladze et al., 2012). Monitoring drug effects can help avoid cancer cells from spreading or developing drug resistance as a result of an ineffective treatment approach. Importantly, we have also recently shown that holographic microscopy has the capacity to identify specific changes in cell phase volume that correlate to either a G1 or a G2/M arrest (Falck Miniotis et al., 2014). In that study, holographic microscopy analysis of average cell phase volume was of comparable accuracy to flow cytometric measurement of cell cycle phase distribution as recorded following dose-dependent treatment with etoposide. We believe that holographic microscopy is an important tool for future image-based analyses of cell volume changes.

5. Conclusion

We demonstrate that morphological changes in cancer cell cultures can be monitored by holographic microscopy. The cell-death induction provides data on decreased cell volume. This can open a new window for personalized medicine investigations, determining the optimal therapeutic concentration for both individual treatment and for different cancer types.

Acknowledgment

This work was supported by grants from the Crafoord Foundation, Malmö University, the Cancer Foundation at Malmö University Hospital, the Magnus Bergvall Foundation, Knut and Alice Wallenbergs Stiftelse, Kungliga fysiografiska sällskapet in Lund, Lars Hierta foundation and Ake Wibergs Stiftelse.

References

Alm, K., El-Schich, Z., Miniotis, M.F., Wingren, A.G., Janicke, B., Oredsson, S., 2013. Cells and Holograms–Holograms and Digital Holographic Microscopy as a Tool to Study the Morphology of Living Cells. In Tech, Rijeka, Croatia.

Carl, D., Kemper, B., Wernicke, G., von Bally, G., 2004. Parameter-optimized digital holographic microscope for high-resolution living-cell analysis. Appl. Opt. 43, 6536–6544.

Chalut, K.J., Ekpenyong, A.E., Clegg, W.L., Melhuish, I.C., Guck, J., 2012. Quantifying cellular differentiation by physical phenotype using digital holographic microscopy. Integr. Biol. 4, 280–284.

Charrière, F., Pavillon, N., Colomb, T., Depeursinge, C., Heger, T.J., Mitchell, E.A., Marquet, P., Rappaz, B., 2006. Living specimen tomography by digital holographic microscopy: morphometry of testate amoeba. Opt. Express 14, 7005–7013.

Cuche, E., Marquet, P., Depeursinge, C., 1999. Simultaneous amplitude-contrast and quantitative phase-contrast microscopy by numerical reconstruction of Fresnel off-axis holograms. Appl. Opt. 38, 6994–7001.

Dubois, F., Yourassowsky, C., Monnom, O., Legros, J.C., Debeir, O., Van Ham, P., Kiss, R., Decaestecker, C., 2006. Digital holographic microscopy for the three-dimensional dynamic analysis of in vitro cancer cell migration. J. Biomed. Opt. 11, 054032.

Falck Miniotis, A., Mukwaya, A., Gjörloff Wingren, A., 2014. Digital holographic microscopy for non-invasive monitoring of cell cycle arrest in L929 cells. PLoS ONE, e0106546.

Ferraro, P., Grilli, S., Alfieri, D., De Nicola, S., Finizio, A., Pierattini, G., Javidi, B., Coppola, G., Striano, V., 2005. Extended focused image in microscopy by digital holography. Opt. Express 13, 6738–6749.

Gustafsson, M., Sebesta, M., 2004. Refractometry of microscopic objects with digital holography. Appl. Opt. 43, 4796–4801.

Gustafsson, M., Sebesta, M., Bengtsson, B., Pettersson, S., Egelberg, P., Lenart, T., 2004. High-resolution digital transmission microscopy—a Fourier holography approach. Opt. Lasers Eng. 41, 553–563.

Jemal, A., Bray, F., Center, M.M., Ferlay, J., Ward, E., Forman, D., 2011. Global cancer statistics. CA Cancer J. Clin. 61, 69–90.

Kemper, B., Carl, D., Schnekenburger, J., Bredebusch, I., Schäfer, M., Domschke, W., von Bally, G., 2006. Investigation of living pancreas tumor cells by digital holographic microscopy. J. Biomed. Opt. 11, 034005–034008.

Ghiglia, D.C., Pritt, M.D., 1998. Two-dimensional phase unwrapping: Theory, algorithms and software. Wiley, New York, USA.

Hawkins, D.H., Abrahamse, H., 2006. The role of laser fluence in cell viability, proliferation, and membrane integrity of wounded human skin fibroblasts following helium-neon laser irradiation. Lasers Surg. Med. 38, 74–83.

Khmaladze, A., Matz, R.L., Epstein, T., Jasensky, J., Banaszak Holl, M.M., Chen, Z., 2012. Cell volume changes during apoptosis monitored in real time using digital holographic microscopy. J. Struct. Biol. 178, 270–278.

Kroemer, G., El-Deiry, W., Golstein, P., Peter, M., Vaux, D., Vandenabeele, P., Zhivotovsky, B., Blagosklonny, M., Malorni, W., Knight, R., 2005. Classification of cell death: recommendations of the Nomenclature Committee on Cell Death. Cell Death Differ. 12, 1463–1467.

Krysko, D.V., Vanden Berghe, T., D'Herde, K., Vandenabeele, P., 2008. Apoptosis and necrosis: detection, discrimination and phagocytosis. Methods 44, 205–221.

Kühn, J., Shaffer, E., Mena, J., Breton, B., Parent, J., Rappaz, B., Chambon, M., Emery, Y., Magistretti, P., Depeursinge, C., 2013. Label-free cytotoxicity screening assay by digital holographic microscopy. Assay Drug Dev. Technol. 11, 101–107.

Logg, K., Bodvard, K., Blomberg, A., Käll, M., 2009. Investigations on light-induced stress in fluorescence microscopy using nuclear localization of the transcription factor Msn2p as a reporter. FEMS Yeast Res. 9, 875–884.

Mann, C., Yu, L., Lo, C., Kim, M., 2005. High-resolution quantitative phase-contrast microscopy by digital holography. Opt. Express 13, 8693–8698.

Miccio, L., Alfieri, D., Grilli, S., Ferraro, P., Finizio, A., De Petrocellis, L., Nicola, S.D., 2007. Direct full compensation of the aberrations in quantitative phase microscopy of thin objects by a single digital hologram. Appl. Phys. Lett. 90, 041104.

Mölder, A., Sebesta, M., Gustafsson, M., Gisselson, L., Wingren, A.G., Alm, K., 2008. Non-invasive, label-free cell counting and quantitative analysis of adherent cells using digital holography. J. Microsc. 232, 240–247.

Pan, F., Liu, S., Wang, Z., Shang, P., Xiao, W., 2012. Digital holographic microscopy long-term and real-time monitoring of cell division and changes under simulated zero gravity. Opt. Express 20, 11496–11505.

Pavillon, N., Kühn, J., Moratal, C., Jourdain, P., Depeursinge, C., Magistretti, P.J., Marquet, P., 2012. Early cell death detection with digital holographic microscopy. PLoS ONE 7, e30912.

Rappaz, B., Marquet, P., Cuche, E., Emery, Y., Depeursinge, C., Magistretti, P., 2005. Measurement of the integral refractive index and dynamic cell morphometry of living cells with digital holographic microscopy. Opt. Express 13, 9361–9373.

Rappaz, B., Breton, B., Shaffer, E., Turcatti, G., 2014. Digital holographic microscopy: a quantitative label-free microscopy technique for phenotypic screening. Comb. Chem. High Throughput Screening 17, 80–88.

Sebesta, M., Gustafsson, M., 2005. Object characterization with refractometric digital Fourier holography. Opt. Lett. 30, 471–473.

Tinevez, J.Y., Dragavon, J., Baba-Aïssa, L., Roux, P., Perret, E., Canivet, A., Galy, V., Shorte, S., 2012. A quantitative method for measuring phototoxicity of a live cell imaging microscope. Methods Enzymol. 506, 292–309.

Wong, R., 2011. Apoptosis in cancer: from pathogenesis to treatment. J. Exp. Clin. Cancer Res. 30, 87–101.

IV

Research Article

For reprint orders, please contact reprints@future-science.com

Future Science OA

Interfacing antibody-based microarrays and digital holography enables label-free detection for loss of cell volume

Background: We introduce the combination of digital holographic microscopy (DHM) and antibody microarrays as a powerful tool to measure morphological changes in specifically antibody-captured cells. The aim of the study was to develop DHM for analysis of cell death of etoposide-treated suspension cells. **Results/Methodology:** We demonstrate that the cell number, mean area, thickness and volume were noninvasively measured by using DHM. The cell number was stable over time, but the two cell lines showed changes of cell area and cell irregularity after treatment. The cell volume in etoposide-treated cells was decreased, whereas untreated cells showed stable volume. **Conclusion:** Our results provide proof of concept for using DHM combined with antibody-based microarray technology for detecting morphological changes in captured cells.

We use an innovative technique that combines digital holographic microscopy and the capture of cells with antibody microarrays as a powerful tool to measure cellular morphological changes. With this technique, the cells can be noninvasively viewed in 3D over time. We obtain results showing changes in cellular parameters including cell area, thickness and volume of the captured cells after treatment with the cell death-inducing drug etoposide. The cell volume in etoposide-treated cells showed a decrease, while untreated cells remained stable. Digital holographic microscopy combined with antibody microarray technology can be a future method for detecting morphological changes in treated cancer cells.

Keywords: antibody • cellular • holography • microarray • volume

Zahra El-Schich[1], Emmy Nilsson[1], Anna S Gerdtsson[2], Christer Wingren[2] & Anette Gjörloff Wingren*[,1]

[1]Department of Biomedical Science, Health & Society, Malmö University, Malmö, Sweden

[2]Department of Immunotechnology & CREATE Health, Medicon Village, Lund University, Lund, Sweden

*Author for correspondence:
Tel.: +46 70 6011857
Fax: +46 40 6658100
anette.gjorloff-wingren@mah.se

The novel technique for noninvasive cell analysis used in this study is label-free and enables qualitative and quantitative measurements of cellular shape and optical thickness [1–10]. Digital holographic microscopy (DHM) have previously been evaluated by us, as a cell counting tool for adherent cells and compared with manual counting with a hemocytometer, showing that the technique was comparable with manual counting, with the additional benefits of being automatic, label-free and not damaging to the cells [3]. The recent development in digital holography has been possible due to technical advances in digital sensors and computers [11]. The holographic principle is based on the phenomenon of interference between wave fronts of coherent light scattered by the object studied and an unaffected (not scattered) reference wave front. In digital holography, a digital sensor (e.g., a CCD-sensor) is used for recording and the reconstruction is performed numerically by computer software [12]. In one recording, three images are taken in three different exposures; the object image, the reference image and the hologram image, which is the interference pattern of the object and the reference light [13]. All information needed for 3D reconstruction is contained in the hologram since the focus depth can be altered to any distance after the image has been taken. By reconstructing the

FUTURE SCIENCE part of fsg

Table 1. Schematic of the array layout and binding of the 13 different single-chain variable antibody fragment fragments directed against two carbohydrates and five different cell surface membrane proteins.

Array row	Specificity	scFv clone	scFv concentration (mg/ml)	Jurkat binding	U2932 binding
1	CD40 ligand	Clone-1	0.20–0.23	-	-
2	LeX	Clone-1	0.20–0.28	++	++
3	LeX	Clone-2	0.20–0.28	++	-
4	LeY	Clone-1	0.20–0.21	-	+
5	Sialyl LeX	Clone-1	0.20–0.24	+	-
6	CD40	Clone-1	0.28–0.40	-	+
7	CD40	Clone-2	0.20–0.26	-	+
8	CD40	Clone-3	0.20–0.24	-	+
9	HLA-DR	Clone-1	0.20–0.24	-	++
10	ICAM-1	Clone-1	0.20–0.26	-	-
11	IgM	Clone-1	0.20–0.28	-	-
12	IgM	Clone-2	0.20–0.28	-	-
13	IgM	Clone-3	0.20–0.26	-	-
14	Phosphate-buffered saline	-	-	-	-

image of the object in multiple adjacent planes the 3D image can hence be built up [12].

The balance between cell growth and controlled cell death is very crucial for many physiological processes [14]. Morphologically, dying cells differ from viable cells in many ways, including cell volume changes. The characteristics of apoptosis are a variety of morphological changes such as loss of cell membrane asymmetry and attachment, cell shrinkage, formation of small blebs, nuclear fragmentation, chromatin condensation and chromosomal DNA fragmentation and finally breakdown of the cell into several apoptotic bodies [15,16]. The most commonly used assays to differentiate between viable and non-viable cells today are trypan blue and propidium iodide staining, both laborious and time-consuming methods. Therefore, DHM is now one of the popular technologies that are used by several groups for cancer cell morphology analyses. DHM has recently been used to measure cell volume changes induced by apoptosis with high time and volume resolution, and in real-time [17]. In another study, excessive stimulation of neurotransmitters through addition of L-glutamate was used to induce cell death in primary cultures of mouse cortical neurons [10]. Cell volume regulation was monitored by DHM phase response which allowed estimation in a very short time-frame, if a neuronal cell would survive or die.

To enable DHM analysis of death-induced suspension cells, we have uniquely added antibody-based microarrays [18] to the experimental set-up. High-performing recombinant antibody microarrays have been developed for immunophenotyping, paving the way for large-scale analysis [19]. Indeed, antibody-based microarray techniques have been used to determine discriminating surface antigen (CD) expression profiles for different B-cell populations and their correlations to discrete leukemia subtypes as well as drug target identification of leukemia cells [20–23]. Moreover, Stybayeva *et al.* recently showed that lensfree holographic imaging combined with antibody microarrays can be used for both characterization of T lymphocytes (CD4 vs CD8) and quantification of cytokine signals [24].

The recombinant antibody-based microarrays were used in this study for specific antigen-capture and immobilization of two selected suspension cell lines, a diffuse large B-cell lymphoma (DLBCL) cell line (U2932) and the T-cell acute lymphoblastic leukemia cell line Jurkat, in combination with subsequent analysis with DHM. Results showed a stable cell number over time for both untreated and treated cells. The cell volume was not changed in untreated cells when analyzed for up to 960 min (16 h), whereas for Jurkat T-cells, the etoposide and dimethyl sulfoxide (DMSO) concentrations used in the study resulted in a decline in cell volume after treatment. For the U2932 B-cells, the etoposide-treatment showed a decrease in cell volume after the same time. The results suggest that DHM is advantageous as a future evaluation tool for suspension cell treatments based on the morphological volume changes accompanying cell death.

Materials & methods

Cell lines

The Jurkat cell line was from ATCC-LGC (LGC Standards, Teddington, Middlesex, UK), whereas U2932 was obtained from Department of Oncology, Genetics and Pathology, Uppsala, Sweden. Both cell lines were maintained in RPMI 1640 (Invitrogen, San Diego, CA, USA) supplemented with 10% fetal calf serum and 50 µg/ml gentamycin (Invitrogen). The cells were cultured in a humidified atmosphere at 37°C with 5% CO_2. A volume of cell suspension containing 2 million cells was centrifuged and thereafter re-suspended in 1 ml phosphate-buffered saline (PBS) with 0.5% (w/v) bovine serum albumin (BSA). The cell suspension containing 200,000 cells/100 µl in PBS with 0.5% (w/v) BSA was applied to an antibody array and incubated at room temperature for 30 min. The array was thereafter washed manually less than equal to ten-times with 100 µl PBS-0.5% BSA each time, until no cells were found outside the antibody functionalized spots, in other words the cell binding areas were clearly visible.

Cell treatment

For each experiment, time-lapse series were run for 960 min (16 h) and holographic imaging was performed every tenth minute. Each experiment was performed at least twice. The experiments were conducted in air without supplemented CO_2 and at room temperature. To avoid drying, a cover glass was attached over the cells. The cell suspension containing 200,000 cells in 100 µl PBS-0.5% BSA was applied to an antibody array and incubated at room temperature for 30 min. After washing, the antibody coated spots 10 which any cells had specifically bound were clearly and distinctly visible. For untreated cells, 30 µl PBS-0.5% BSA was added to the adhered cells. For treated cells, either 30 µl of 10% DMSO, or 30 µl of 500 µM etoposide (Sigma-Aldrich Co., MO, USA) in PBS-0.5% BSA was added to the array before covering.

Antibody microarrays

Recombinant antibody arrays containing 13 different single-chain variable antibody fragments (scFv) [25] against five different cell surface membrane proteins and two carbohydrates, plus a negative control (PBS) were immobilized to silane-coated glass slides (Sigma-Aldrich) through passive adsorption. The scFv antibodies were selected from a large phage display library. This library represents a renewable antibody source, and the antibodies have been designed for microarray applications by molecular design, thus displaying high-on chip performance (e.g., stability, reproducibility, functionality and specificity). The probe source (format) has been found to display superior on-chip performances compared with conventional monoclonal and polyclonal antibodies [25,26]. The specific

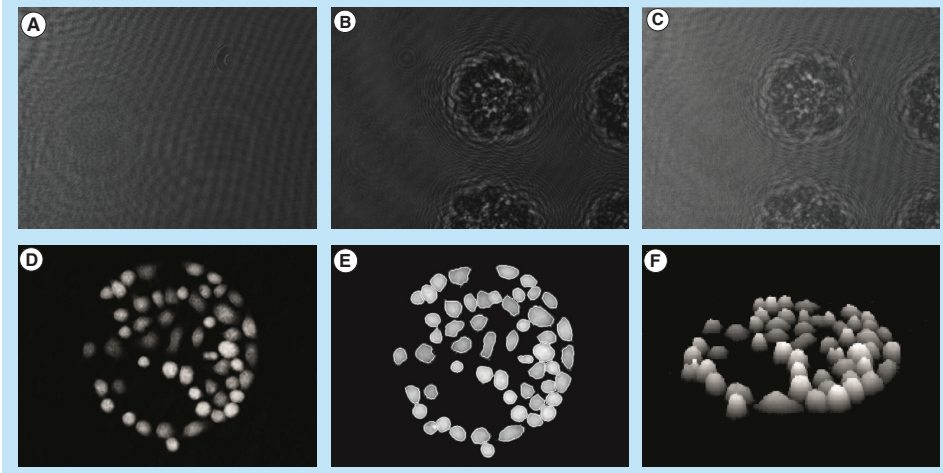

Figure 1. Jurkat cells captured on antibody Lewis X Clone-1. (A) Reference diffraction pattern; **(B)** object diffraction pattern and **(C)** hologram diffraction pattern; **(D)** numerical reconstruction of the hologram rendered the 3D image of the cells; **(E)** segmentation algorithm marked each individual cell; and **(F)** 3D image of the Jurkat cells.

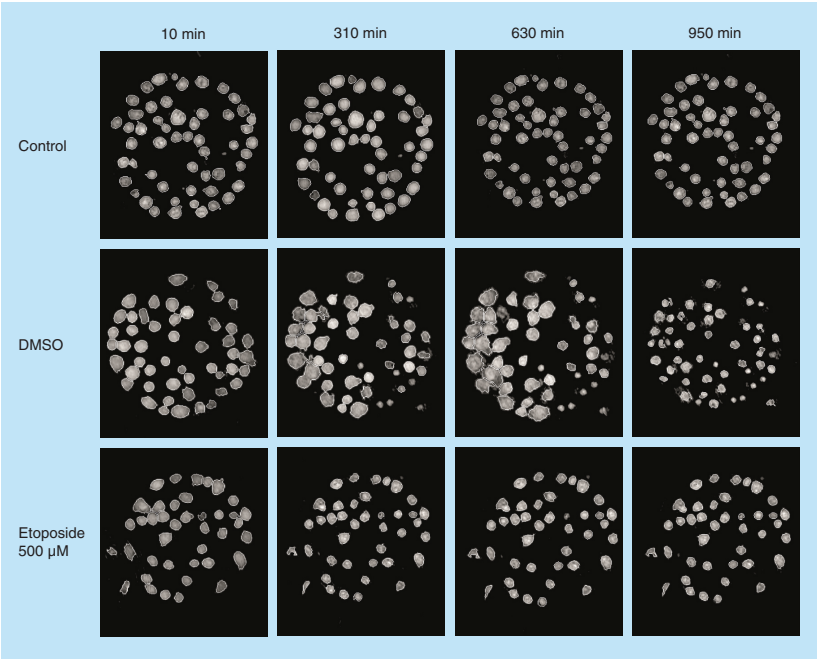

Figure 2. Hologram images of Jurkat cells captured on antibody Lewis X Clone-1. The images are showing control, DMSO and etoposide-treated cells at four different timepoints: 10, 310, 630 and 950 min. The cells are segmented to analyze cell parameters.
DMSO: Dimethyl sulfoxide.

13 antibodies used in this study were selected based on the criteria that they were tested to work well in microarray applications and directed against target antigens located in the cell surface membrane [19,27,28]. More specifically, we use recombinant scFv antibodies that have been designed for microarray applications by molecular design, thus displaying high-on chip performance. The scFv antibodies can target both high- and low-abundant (pM to fM range) analytes in crude nonfractionated proteomes in a highly specific and reproducible manner (CV < 10%). The scFv antibodies were produced in *Escherichia coli* and purified using Ni^{2+}-NTA affinity chromatography as described elsewhere [29].

The purified antibodies were stored in PBS at 4°C until use. The arrays were produced by dispensing 300 pl antibody solution (0.24 ± 0.35 mg/ml) in discrete positions using the noncontact inkjet printer Sci Flexarrayer S11 (Scienion AG, Berlin, Germany). In this study, we printed four subarrays per slide, and each subarray was composed of 14 × 8 individual spots, meaning that 13 antibodies + 1 control was spotted in eight replicates.

Microscope & software

For cell imaging the HoloMonitor™ M2 (Phase Holographic Imaging AB, Lund, Sweden) was used, which combines both phase contrast microscopy and digital holography. It uses a 0.8 mW HeNe laser (633 nm) with an intensity of approximately 10 Wm^{-2}. The exposure time during imaging was less than 3 ms which assures insensitivity to vibrations and minimal physiological effects on cell function. The image algorithm HoloStudio (Phase Holographic Imaging AB) was used to analyze different cell parameters, for example, cell area, cell thickness and cell volume, as described elsewhere [3,6–8].

Results

Antibody binding of Jurkat & U2932 cells

The degree of cell binding to the arrayed antibodies was first studied using phase contrast microscopy (Table 1). One cell binding antibody area was selected for holo-

graphic photography. The antibody area was selected based on representative cell binding and number of cells bound, over several trials. The number of cells that bound to each antibody spot varied between about 25 and 65, but most spots contained 30 to 40 specifically captured cells. The last criterion was included to avoid two cells being segmented as one because of too close binding. The consistency in the binding patterns could hence be noticed. The Jurkat cells bound to the Lewis X Clone-1 and Clone-2 antibodies and sometimes a weak binding to sialyl Lewis X antibodies could be observed. For Jurkat cells Lewis X Clone-1 antibody was used for holographic measurements. U2932 cells bound consistently to Lewis X Clone-1 and HLA-DR antibodies and in some cases also to CD40 and Lewis Y antibodies. When imaging U2932 cells, HLA-DR or Lewis Y antibody spots were selected.

Image acquisition & analysis of cell properties

For each time point of holographic measurements, three images were obtained: the object wave image, the reference wave image and the hologram image, which is the interference pattern of the former two, as shown for untreated Jurkat cells (Figure 1A–C). A 'height map' (Figure 1D), was performed by the computer software, which subsequently used a segmentation algorithm to find the individual cells enabling analysis of cell parameters (Figure 1E). The segmentation process most often succeeded well in dividing between adjacent cells, but for some samples the focus had to be reset manually to make the image sharp enough for segmentation or the segmentation parameters (e.g., threshold for core thickness) had to be adjusted. Numerical reconstruction of holograms into a 3D image (Figure 1F) was performed by the computer software which subsequently used a segmentation algorithm to find the individual cells enabling analysis of cell parameters.

Analysis of cell holograms

To investigate the cellular responsiveness, Jurkat and U2932 cells were treated with etoposide, DMSO or

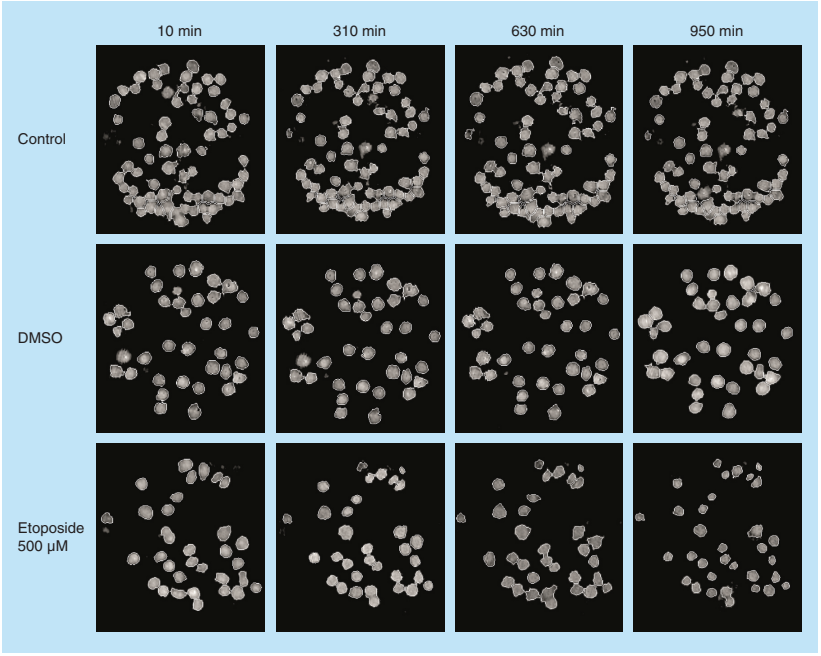

Figure 3. Hologram images of U2932 cells captured on antibody HLA-DR. The images are showing control, DMSO and etoposide-treated cells at four different timepoints: 10, 310, 630 and 950 min. The cells are segmented to analyze cell parameters.
DMSO: Dimethyl sulfoxide.

left untreated and a cover glass was added to avoid evaporation and keep concentrations constant. Holograms were collected every tenth minute for a period of 16 h. To show images of the holograms after segmentation, four different time points were chosen for Jurkat cells and U2932 cells, respectively. Jurkat cells captured on antibody Lewis X Clone-1 are displayed as control, DMSO and etoposide-treated cells at the time-points 10, 310, 630 and 950 min (Figure 2). An enlargement of the cell area is seen in Jurkat cells after DMSO-treatment. U2932 cells captured on antibody HLA-DR are displayed as control, DMSO and etoposide-treated cells at the timepoints 10, 310, 630 and 950 min (Figure 3).

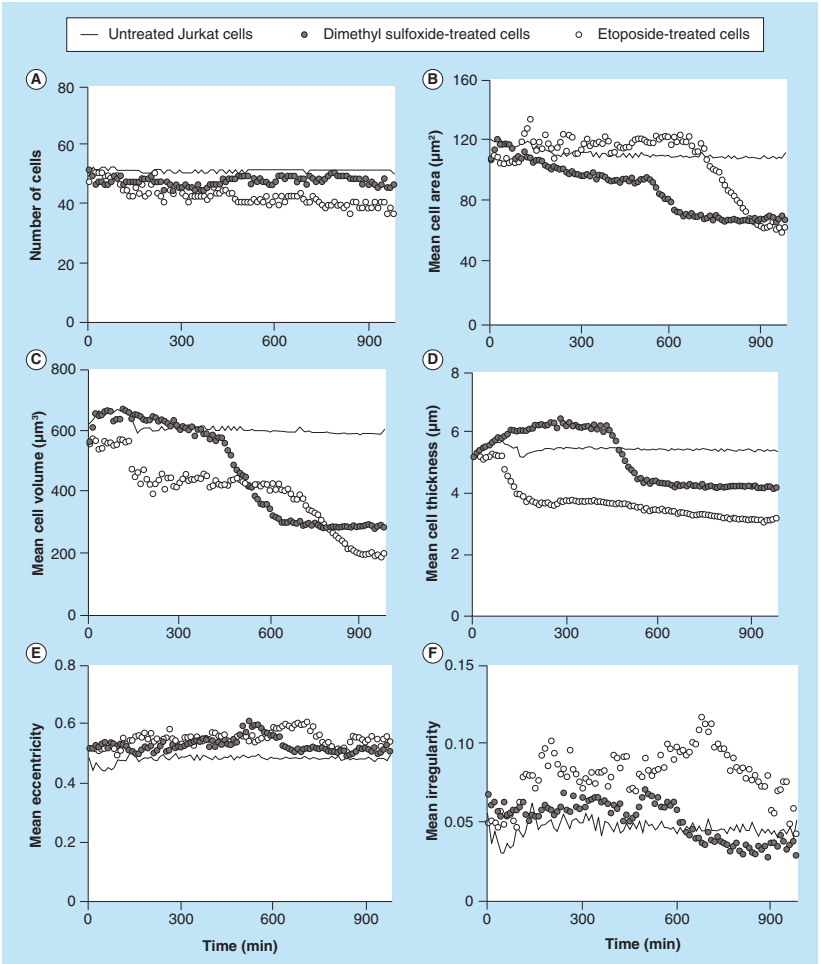

Figure 4. Different cellular parameters of treated (etoposide or dimethyl sulfoxide) or untreated Jurkat cells captured on antibody Lewis X Clone-1 were analyzed over time. (A) Number of cells; **(B)** mean cell area; **(C)** mean cell volume; **(D)** mean cell thickness; **(E)** mean cell eccentricity; and **(F)** mean cell irregularity.

Analysis of cell parameters

Data for cell number, cell area, cell thickness, cell volume, cell eccentricity and cell irregularity were collected and the results for the different treatments of Jurkat and U2932 were plotted versus time. Untreated Jurkat cells showed stable cell number over the time period (Figure 4A). The mean cell area for untreated Jurkat cells was also stable and was measured to 110–120 μm^2 (Figure 4B). When treating the Jurkat cells with either the solvent DMSO or high concentrations of etoposide (500 μM), the mean cell area became unstable. The DMSO treatment initially resulted in an increase of the cell area (also seen in Figure 2), and with time a decrease down to 60–70 μm^2, which was similar to the final mean cell area of etoposide-treated Jurkat cells. The mean cell volume was initially around 600 μm^3. The volume of DMSO-treated cells decreased much faster than etoposide-treated cells, but after about 800 min, the cells have reached about the same decrease in mean cell volume. The mean eccentricity of the cells does not show any major variations (Figure 4E), whereas an increase in the mean cellular irregularity was more pronounced for DMSO-treated cells (Figure 4F).

Interestingly, the U2932 cells showed a somewhat different pattern compared with the Jurkat cells. First, the untreated U2932 cells showed stable cell number over the time period (Figure 5A), but the cell number for the treated U2932 cells were lower from the beginning of the experiment (also seen in Figure 3). The mean cell area for the U2932 cells was slightly smaller compared with the area of the Jurkat cells (Figure 5B). The DMSO-treatment resulted in a fast increase of the cell area, but at a later time point the area decreased. The etoposide-treatment resulted in a later increase of the cell area (600 min), which finally declined. The mean cell thickness and volume of treated U2932 cells showed initially a slight increase (Figure 5C). Over the time period of measurement, only the etoposide-treated U2932 cells showed a change in cell volume from 600 μm^3 down to 200 μm^3. The mean eccentricity of the U2932 cells does not show any major variations (Figure 5E), whereas etoposide-treated cells showed a peak in increased mean cellular irregularity between 600 and 900 min. (Figure 5F).Taken together, we showed for the first time that DHM in combination with antibody microarrays could be used to analyze treated nonadherent DLBCL and T-cell acute lymphoblastic leukemia cells in real time.

Discussion

Development of fast and accurate evaluation tools for cancer treatments will be of great value to clinicians in deciding the most appropriate treatment for patients. The novel technology of DHM uniquely combined with recombinant antibody microarrays presented here provides a whole new ability of specific capture of suspension cells and determination of qualitative and quantitative cellular parameters, combined with a subsequent in real time analysis of induced morphological changes after treatment with cell-death inducing agents. In this study, we have used DHM for determining the cell area, thickness and volume to evaluate the cell death progression in suspension cell lines treated with either etoposide or the solvent DMSO. Experiments were conducted over night with a cover glass attached on top of the antibody microarray to minimize evaporation. Untreated controls for both U2932 and Jurkat cells showed very good stability for measurements up to 16 h, with no changes in the measured cell number. Furthermore, no notable detachment of cells from the antibodies could be detected. The adhesion profile is in agreement with a previous study using the DHM, where U2932 cells were found to adhere strongly to antibodies binding to HLA-DR and Lewis X antibodies (unpublished results). For control cells, the mean cell area, thickness and volume measurements were stable.

Both cell lines were treated with high concentrations of etoposide for induction of fast morphological changes. Changes in cell volume are associated with both normal cellular processes such as proliferation and cell cycle regulation, but also associated with programed cell death [17]. Here, we show that the cell volume of etoposide-treated Jurkat cells and U2932 cells decreases 2–3 h after initiating the treatment. For U2932 cells, the decrease in cell thickness after etoposide-treatment was prominent and also affects the overall cell volume decrease. Etoposide causes errors in the DNA synthesis and promotes apoptosis of the cancer cell by forming a ternary complex with DNA and the enzyme topoisomerase II [30]. Interestingly, the solvent DMSO also resulted in prominent swelling of the Jurkat cells, quite in contrast to the outcome of the U2932 cells.

We also show novel results on the morphological cell parameters eccentricity and irregularity. Interestingly, the Jurkat cells showed a high degree of irregularity after DMSO-treatment. In contrast, the etoposide-treated U2932 cells showed a peak in both cellular eccentricity (unconventional or irregular behavior) and cellular irregularity after 600 min of treatment, indicating the possibility to measure morphological changes at any time point during DHM analysis.

The interest for analyzing cell volume changes of adherent cells with DHM as a result of cytotoxicity or apoptosis treatment has recently increased in popularity [10,17,31–33]. Hematological neoplasms, such as leukemia and lymphoma, are examples of diseases that

could benefit from development of the DHM technique. There are many different subtypes of hematological malignancies and several different techniques are used to classify samples from patients, for example, morphology, pathological studies, immunophenotyping, cytogenetics and molecular genetics [34,35]. Although significant advances in diagnostics have been made during the last decades, there are still difficulties with stratification of important disease categories such as DLBCL and follicular lymphoma.

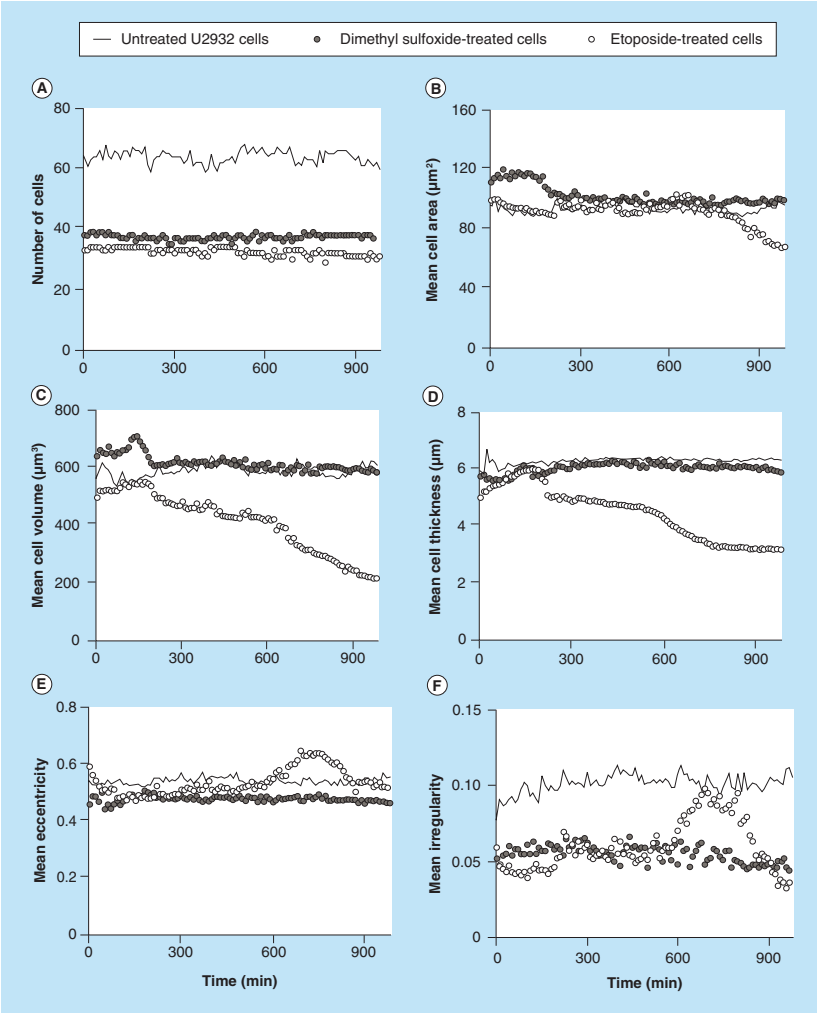

Figure 5. Different cellular parameters of treated (etoposide or dimethyl sulfoxide) or untreated U2932 cells captured on antibody HLA-DR were analyzed over time. (A) Number of cells; **(B)** mean cell area; **(C)** mean cell volume; **(D)** mean cell thickness; **(E)** mean cell eccentricity; and **(F)** mean cell irregularity.

In conclusion, we have provided evidence that suspension cells specifically captured by recombinant antibody-based microarrays, either individual cells or cell populations, could be monitored in real time directly on glass slides, and morphological parameters such as cell area, thickness, volume and irregularity could readily monitored and analyzed.

Conclusion & future perspective

Different subclasses of leukemia and lymphoma need different treatment protocols involving chemotherapy, radiation therapy and bone marrow stem cell transplantation and the prognosis for different diagnoses is also varying. To improve the outcome for patients with hematological malignancies, new therapies are required, but as a correct diagnosis is crucial for the choice of treatment and hence the outcome. There is also an urgent need for fast and more accurate diagnostic tools. Considerable progress has been made in the DHM field in the past few years, and the use of DHM combined with antibody microarrays as a fast, automatic and cost efficient evaluation tool for different cancer treatments looks promising.

Financial & competing interests disclosure

The authors would like to thank Malmö University, the Crafoord foundation, the Swedish Research Council (VR-NT) and The Cancer Foundation at Malmö University Hospital for support. The authors have no other relevant affiliations or financial involvement with any organization or entity with a financial interest in or financial conflict with the subject matter or materials discussed in the manuscript apart from those disclosed.

No writing assistance was utilized in the production of this manuscript.

Ethical conduct

The authors state that they have obtained appropriate institutional review board approval or have followed the principles outlined in the Declaration of Helsinki for all human or animal experimental investigations. In addition, for investigations involving human subjects, informed consent has been obtained from the participants involved.

Executive summary

- Suspension cell lines can be captured to antibody-based microarrays and thereafter measured for cell number, mean cell area, thickness and volume using digital holographic microscopy.
- The cell number was stable over time and the two cell lines showed cell-specific results of cell area and cell irregularity after treatment.
- The cell volume could be analyzed in cells treated for up to 16 h, showing a decrease in both cell lines, whereas untreated cells showed stable volume.
- Our results provide support for using the concept of digital holography combined with antibody-based microarray technology as a novel method for detecting morphological changes in specifically captured death-induced cells.

References

Papers of special note have been highlighted as:
• of interest; •• of considerable interest

1 Marquet P, Rappaz B, Magistretti PJ. Digital holographic microscopy: a noninvasive contrast imaging technique allowing quantitative visualization of living cells with subwavelength axial accuracy. *Opt. Lett.* 30(5), 468–470 (2005).

• **Illustrates how the technique of digital holography opens up new perspectives within biomedical applications by enable both qualitative and quantitative label-free live cell imaging by the information from one single hologram.**

2 Rappaz B, Marquet P, Cuche E *et al.* Measurement of the integral refractive index and dynamic cell morphometry of living cells with digital holographic microscopy. *Opt. Express* 13(23), 9361–9373 (2005).

•• **Presents results of how cortical neurons from mouse embryonical cells in primary cultures were treated with a hypotonic solution and analyzed. The optical phase shift was determined, and found to be either increasing or decreasing in different parts of the cells.**

3 Mölder A, Sebesta M, Gustafsson M *et al.* Non-invasive, label-free cell counting and quantitative analysis of adherent cells using digital holography. *J. Microscopy* 232(2), 240–247 (2008).

4 Yu L, Mohanty S, Zhang J *et al.* Digital holographic microscopy for quantitative cell dynamic evaluation during laser microsurgery. *Opt. Express* 17(14), 12031–12038 (2009).

5 Kemper B, Bauwens A, Vollmer A *et al.* Label-free quantitative cell division monitoring of endothelial cells by digital holographic microscopy. *J. Biomed. Opt.* 15(3), 036009 (2010).

6 Persson J, Mölder A, Pettersson SG, Alm K. Cell motility studies using digital holographic microscopy In: *Microscopy: Science, Technology, Applications and Education*. Méndez-Vilas A, Díaz Álvarez J (Eds). Formatex Research Center, Badajoz, Spain, 1063–1072 (2010).

7 Alm K, Cirenajwis H, Gisselsson L *et al.* Digital holography and Cell Studies. In: *Holography, Research and Technologies.* Rosen J (Ed.). In Tech, Rijeka, Croatia, 237–252 (2011).

8 El-Schish Z, Mölder A, Sebesta M *et al.* Digital holographic microscopy – innovative and non-destructive analysis of living cells In: *Microscopy: Science, Technology, Applications and Education*. Méndez-Vilas A, Díaz Álvarez J (Eds). Formatex Research Center, Badajoz, Spain, 1055–1062 (2010).

9 Mihailescu M, Scarlat M, Gheorghiu A *et al.* Automated imaging, identification, and counting of similar cells from digital hologram reconstructions. *Appl. Opt.* 50(20), 3589–3597 (2011).

10 Pavillon N, Kühn J, Moratal C *et al.* Early cell death detection with digital holographic microscopy. *PLoS ONE* 7(1), e30912 (2012).

•• **Describes how cell volume regulation was monitored by digital holographic microscopy (DHM) phase response. By monitoring the phase shift, the authors were able to distinguish nuclear condensation and 'blebbing' induced by treatment which could indicate that cells were apoptotic rather than necrotic.**

11 Sebesta M, Gustafsson M. Object characterization with refractometric digital Fourier holography. *Opt. Lett.* 30(5), 471–473 (2005).

12 Garcia-Sucerquia J, Xu W, Jericho SK *et al.* Digital in-line holographic microscopy. *Appl. Opt.* 45(5), 836–850 (2006).

13 Lenart T, Gustafsson M, Öwall V. A hardware acceleration platform for digital holographic imaging. *J. Sign. Process Syst.* 52(3), 297–311 (2008).

14 Reed JC. Mechanisms of apoptosis. *Am. J. Pathol.* 157(5), 1415–1430 (2000).

15 Bortner CD, Sifre MI, Cidlowski JA. Cationic gradient reversal and cytoskeleton-independent volume regulatory pathways define an early stage of apoptosis. *J. Biol. Chem.* 283(11), 7219–7229 (2008).

16 Kroemer G, Galluzzi L, Vandenabeele P *et al.* Classification of Cell Death: Recommendations of the Nomenclature Committee on Cell Death. *Cell Death Diff.* 16(1), 3–11 (2009).

17 Khmaladze A, Matz RL, Epstein T *et al.* Cell volume changes during apoptosis monitored in real time using digital holographic microscopy. *J. Struct. Biol.* 178(3), 270–278 (2012).

• **Illustrates how an early stage morphological feature of apoptosis was observed in treated cells – a marked decrease in cell volume. The ability to analyze individual cells in a given cell population by using DHM was successfully demonstrated, as individual treatment-induced cell responses could be monitored. The authors showed time-dependent fluctuations in cell volume, which increased in the earlier phases of treatment.**

18 Wingren C, James P, Borrebaeck CAK. Strategy for surveying the proteome using affinity proteomics and mass spectrometry. *J. Proteomics* 9(6), 1511–1517 (2009).

19 Dexlin L, Ingvarsson J, Frendéus B *et al.* Design of recombinant antibody microarrays for cell surface membrane proteomics. *J. Proteome Res.* 7(1), 319–327 (2008).

20 Belov L, Mulligan SP, Barber N *et al.* Analysis of human leukaemias and lymphomas using extensive immunophenotypes from an antibody microarray. *Br. J. Haematol.* 135(2), 184–197 (2006).

21 Ellmark P, Högerkorp CM, Ek S *et al.* Phenotypic protein profiling of different B cell sub-populations using antibody CD-microarrays. *Cancer Lett.* 265(1), 98–106 (2008).

22 Barber N, Gez S, Belov L *et al.* Profiling CD antigens on leukaemias with an antibody microarray. *FEBS Lett.* 583(11), 1785–1791 (2009).

23 Kohnke, PL, Mulligan, SP, Christopherson, R.I. Membrane proteomics for leukemia classification and drug target identification. *Curr. Opin. Mol. Ther.* 11(6), 603–610 (2009).

24 Stybayeva G, Mudanyali O, Seo S *et al.* Lensfree holographic imaging of antibody microarrays for high-throughput detection of leukocyte numbers and function. *Anal. Chem.* 82(9), 3736–3744 (2010).

25 Borrebaeck CAK, Wingren C. Recombinant antibodies for the generation of antibody arrays. In: *Protein Microarrays: Methods in Molecular Biology.* Korf U (Ed.). Humana Press Inc., New York, NY, USA, 785, 247–262 (2011).

26 Borrebaeck CAK, Wingren C. Design of high-density antibody microarrays for disease proteomics: key technological issues. *J. Proteomics* 72(6), 928–935 (2009).

27 Dexlin-Mellby L, Sandström A, Antberg L *et al. et al.* Design of recombinant antibody microarrays for membrane protein profiling of cell lysates and tissue extracts. *Proteomics* 11(8), 1550–1554 (2011).

28 Dexlin-Mellby L, Sandström A, Centlow M *et al.* Tissue proteome profiling of preeclamptic placenta using recombinant antibody microarrays. *Proteomics Clin. Appl.* 4(10–11), 794–807 (2010).

29 Carlsson A, Wuttge DM, Ingvarsson J *et al.* Serum protein profiling of systemic lupus erythematosus and systemic sclerosis using recombinant antibody microarrays. *Mol. Cell. Proteomics* 10(5), M110.005033 (2011).

30 Montecucco A, Biamonti G. Cellular response to etoposide treatment. *Cancer Lett.* 252(1), 9–18 (2007).

31 Trulsson M, Yu H, Gisselsson L *et al.* HAMLET binding to α-actinin facilitates tumor cell detachment. *PLoS ONE* 6(3), e17179 (2011).

32 Kühn J, Shaffer E, Mena J *et al.* Label-free cytotoxicity screening assay by digital holographic microscopy. *Assay Drug Dev. Technol.* 11(2), 101–107 (2013).

• **Validates the use of DHM for monitoring morphological cell changes. The experimental outputs of this technique is compared with standard fluorescence microscopy methods. This is also the first demonstration and quantitative assessment of the applicability of DHM for image-based cellular screening in 96-well-plate format.**

33 Wang Y, Yang Y, Wang D *et al.* Morphological measurement of living cells in methanol with digital

holographic microscopy. *Comput. Math. Methods Med.* 1–7 (2013).

34 Jaffe E.S. The 2008 WHO classification of lymphomas: implications for clinical practice and translational research. *Hematology* 1, 523–531 (2009).

35 Bacher U., Schnittger S., Haferlach C *et al.* Molecular diagnostics in acute leukemias. *Clin. Chem. Lab. Med.* 47(11), 1333–1341 (2009).

Malmö University Health and Society Doctoral Dissertations

Ross, M. W. Typing, doing and being. A study of men who have sex with men and sexuality on the Internet. 2006:1

Stoltz, P. Searching for meaning of support in nursing. A study on support in family care of frail aged persons with examples from palliative care at home. 2006:2

Gudmundsson, P. Detection of myocardial ischemia using real-time myocardial contrasts echocardiography. 2006:3

Holmberg, L. Communication in palliative home care, grief and bereavement. A mother's experiences. 2007:1

Ny, P. Swedish maternal health care in a multiethnic society – including the fathers. 2007:2

Schölin, T. Etnisk mångfald som organisationsidé. Chefs- och personalpraktiker i äldreomsorgen. 2008:1

Svensson, O. Interactions of mucins with biopolymers and drug delivery particles. 2008:2

Holst, M. Self-care behaviour and daily life experiences in patients with chronic heart failure. 2008:3

Bahtsevani, C. In search of evidence-based practices. Exploring factors influencing evidence-based practice and implementation of clinical practice guidelines. 2008:4

Andersson, L. Endocytosis by human dendritic cells. 2009:1.

Svendsen, I. E. *In vitro* and *in vivo* studies of salivary films at solid/liquid interfaces. 2009:2.

Persson, K. Oral health in an outpatient psychiatric population. Oral status, life satisfaction and support. 2009:3.

Hellman, P. Human dendritic cells. A study of early events during pathogen recognition and antigen endocytosis. 2009:4.

Baghir-Zada, R. Illegal aliens and health (care) wants. The cases of Sweden and the Netherlands. 2009:5.

Stjernswärd, S. Designing online support for families living with depression. 2009:6.

Carlsson, A. Child injuries at home – prevention, precautions and intervention with focus on scalds. 2010:1.

Carlson, E. Sjuksköterskan som handledare. Innehåll i och förutsättningar för sjuksköterskors handledande funktion i verksamhetsförlagd utbildning – en etnografisk studie. 2010:2.

Sinkiewicz, G. *Lactobacillus reuteri* in health and disease. 2010:3.

Tuvesson, H. Psychiatric nursing staff and the workplace. Perceptions of the ward atmosphere, psychosocial work environment, and stress. 2011:1.

Ingvarsdotter, K. Mental ill health and diversity. Researching human suffering and resilience in a multicultural context. 2011:2.

Hamit-Eminovski, J. Interactions of biopolymers and metal complexes at biological interfaces. 2011:3.

Mellgren, C. What´s neighbourhood got to do with it? The influence of neighbourhood context on crime and reactions to crime. 2011:4.

Annersten Gershater, M. Prevention of foot ulcers in patients with diabetes mellitus. Nursing in outpatient settings. 2011:5.
Pooremamali P. Culture, occupation and occupational therapy in a mental care context- the challenge of meeting the needs of Middle Eastern immigrants. 2012:1

Gustafsson A. Aspects on sepsis: treatment and markers. 2012:2

Lavant, E. Multiplex HLA-DR-DQ genotyping. For genetic epidemiology and clinical risk assessment. 2012:3

Wangel, A-M. Mental ill-health in childbearing women. Markers and risk factors. 2012:4

Scaramuzzino, R. Equal opportunities? - A cross-national comparison of immigrant organisations in Sweden and Italy. 2012:5

Ivert, A-K. Adolescent mental health and utilisation of psychiatric care - The role of parental country of birth and neighbourhood of residence 2013:1

Znamenskaya, Y. Effect of hydration on thermodynamic, rheological and structural properties of mucin. 2013:2

Andersson, F. The female offender. Patterning of antisocial and criminal activity over the life-course. 2013:3

Lindroth, M. Utsatthet och sexuell hälsa – en studie om unga på statliga ungdomshem. 2013:4

Hulusjö, A. The multiplicities of prostitution experience – narratives about power and resistance. 2013:5

Falk, M. Direct electron transfer based biofuel cells. Operation in vitro and in vivo. 2014:1

Finnbogadóttir, H. Exposure to domestic violence during pregnancy. Impact on outcome, midwives' awareness, women´s experience and prevalence in the south of Sweden. 2014:2
Fagerström, A. Effects of surfactant adjuvants on barrier properties of plant leaf cuticle. 2014:3

Lamberg, P. Design and characterization of direct electron transfer based biofuel cells including tests in cell cultures. 2014:4

Richert, T. Överdoser, försörjningsstrategier och riskhantering – livsvillkor för personer som injicerar narkotika. 2014:5

Örmon, K. Experiences of abuse during the life course. - Disclosure and the care provided among women in a general psychiatric context. 2014:6

Sjöblom, I. Planerade hemförlossningar i Norden - kvinnors och barnmorskors perspektiv. 2014:7

Albèr, C. Humectants and Skin - Effects of hydration from molecule to man. 2015:1

Kisch M., A. Allogeneic stem cell transplantation. – Patients' and sibling donors' perspectives. 2015:2

Weiber, I. Children in families where the mother has an intellectual or developmental disability – incidence, support and first person perspectives. 2015:3

Schlyter, M. Myocardial infarction, Personality factors, Coping strategies, Depression and Secondary prevention 2016:1

Carlström, C. BDSM – Paradoxernas praktiker. 2016:2

El-Schich, Z. Novel imaging technology and tools for biomarker detection in cancer. 2016:3

The publications are available on-line.
See www.mah.se/muep

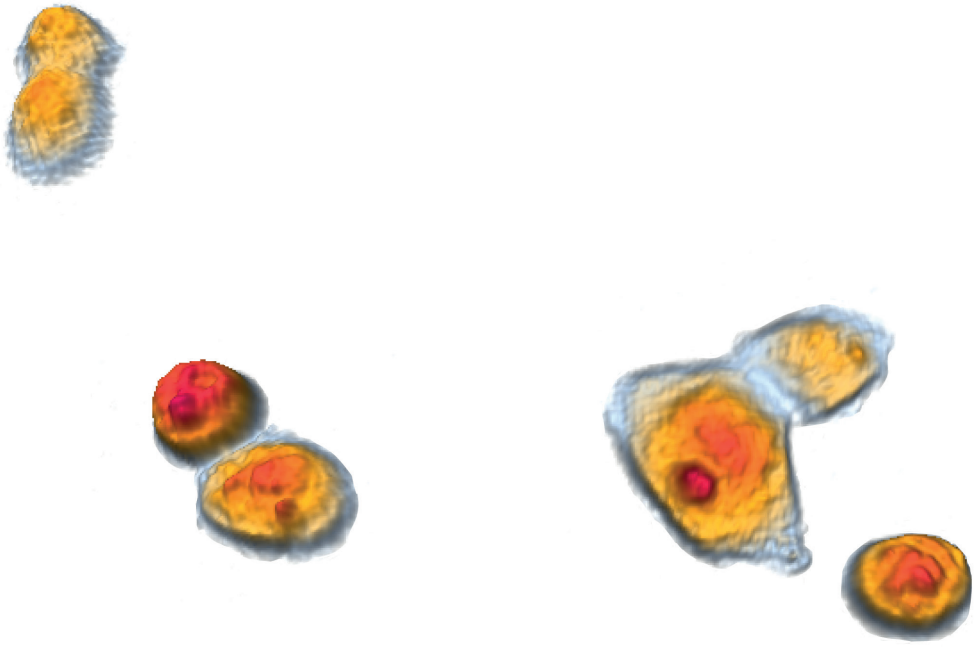

ISBN 978-91-7104-660-4 (print)
ISBN 978-91-7104-661-1 (pdf)
ISSN 1653-5383

MALMÖ HÖGSKOLA
205 06 MALMÖ, SWEDEN
WWW.MAH.SE